

# Identification of Novel GPR55 Modulators Using Cell-Impedance-Based Label-Free Technology

*Paula Morales,<sup>#</sup> Lauren Whyte,<sup>¶</sup> Roberto Chicharro,<sup>#,†</sup> María Gómez-Cañas,<sup>§,§,£</sup> M. Ruth Pazos,  
<sup>§,§,£</sup> Pilar Goya,<sup>#</sup> Andrew J. Irving,<sup>‡</sup> Javier Fernández-Ruiz,<sup>§,§,£</sup> Ruth A. Ross,<sup>¶,\*</sup> and Nadine  
Jagerovic<sup>#,\*</sup>*

<sup>#</sup> Instituto de Química Médica, CSIC, Calle Juan de la Cierva, 3, 28006 Madrid, Spain

<sup>¶</sup> Department of Pharmacology and Toxicology, Medical Sciences Building, University of  
Toronto, 1 King's College Circle, Toronto, Ontario, M5S 1A8, Canada

<sup>§</sup> Departamento de Bioquímica y Biología Molecular, Facultad de Medicina, Universidad  
Complutense de Madrid, 28040 Madrid, Spain

<sup>§</sup> Centro de Investigación Biomédica en Red sobre Enfermedades Neurodegenerativas  
(CIBERNED), 28040 Madrid, Spain

<sup>£</sup> Instituto Ramón y Cajal de Investigaciones Sanitarias (IRYCIS), Madrid, Spain

<sup>‡</sup> School of Biomolecular and Biomedical Science, University College Dublin, Dublin D4,  
Ireland

KEYWORDS. GPR55; cannabinoid; cell impedance; GPR55 agonist; GPR55 antagonist; chromenopyrazole.

ABSTRACT: The orphan G protein-coupled receptor GPR55 has been proposed as a novel receptor of the endocannabinoid system. However, the validity of this categorization is still under debate mainly due to the lack of potent and selective agonists and antagonists of GPR55. Binding assays are not yet available for GPR55 screening and GPR55 signal pathways discrepancies have been reported. In this context, we have designed and synthesized novel GPR55 ligands based on a chromenopyrazole scaffold. Appraisal of GPR55 activity was accomplished by a label-free cell-impedance based assay using GPR55-HEK293. The real-time impedance responses provide an integrative assessment of the cellular consequence to GPR55 stimulation taking into account the different possible signaling pathways. Potent GPR55 partial agonists (**14b**, **18b**, **19b**, **20b**, and **21–24**) have been identified; one of them (**14b**) being selective *vs* classical cannabinoid receptors. Upon antagonist treatment, the chromenopyrazoles **21–24** inhibited lysophosphatidylinositol (LPI) effect. One of these GPR55 antagonists (**21**) is fully selective *vs* classic cannabinoid receptors. Compared to LPI, predicted physicochemical parameters of the new compounds suggest a clear pharmacokinetic improvement.

## INTRODUCTION

The orphan G-protein coupled receptor (GPCR) GPR55 was first cloned and identified in 1999 by O'Dowd and collaborators.<sup>1</sup> A few years later, screening assays carried out on cannabinoid libraries by AstraZeneca<sup>2</sup> and GlaxoSmithKline<sup>3</sup> revealed that GPR55 might be activated by some endogenous, natural and synthetic cannabinoid ligands. Since the complex pharmacology of the endocannabinoid system points to the existence of new physiologically-relevant receptor types for these signaling lipids other than classic cannabinoid receptors (CBRs), GPR55 was presented as one of the missing cannabinoid receptor types.<sup>4-13</sup> However, the validity of this categorization is being extensively discussed mainly due to the GPR55 complex cellular signaling pathways, as well as due to the lack of useful selective ligands for investigating GPR55 biological functions.

Structurally, GPR55 is a seven transmembrane receptor that belongs to the  $\delta$  group of rhodopsin-like GPCRs (Class A). Human GPR55 (hGPR55) is formed by a 319 amino acids sequence that shares low identity with the CBRs described so far, CB<sub>1</sub>R and CB<sub>2</sub>R (13.5% and 14.4% respectively). The GPCR proteins most homologous with GPR55 are GPR35 (27%), P2Y (29%), GPR23 (30%), CCR4 (23%), LPA4 (30%) and LPA5 (30%).<sup>1,14</sup>

Despite the potential therapeutic interest of GPR55 in inflammatory processes,<sup>15</sup> metabolic regulation,<sup>16</sup> vascular functions,<sup>17</sup> bone resorption,<sup>18</sup> and cancer cell proliferation, migration, and invasion,<sup>19-21</sup> the design of potent and selective GPR55 ligands remains, as mentioned above, a major challenge for medicinal chemists.<sup>5</sup> Lysophosphatidylinositol (LPI) has been confirmed as a GPR55 agonist in various cellular systems with pharmacological outcomes, and it has been proposed as the putative endogenous ligand of GPR55.<sup>22-26</sup> Furthermore, various endogenous cannabinoid ligands have been identified as potential GPR55 modulators. However, there are

discrepancies between the diverse studies. For instance, 2-arachidonoylglycerol (2-AG) showed agonist efficacy in [<sup>35</sup>S]GTPγS binding assay, but it was ineffective in β-arrestin recruitment and GPR55 internalization.<sup>10</sup> Bioactive constituents from the plant *Cannabis Sativa* (e.g., tetrahydrocannabinol (Δ<sup>9</sup>-THC))<sup>25,27</sup> and synthetic analogues (e.g., HU210, abnormal-cannabidiol (ABN-CBD), CP55,940, SR141716A) have also shown conflicting data in relation with their GPR55 pharmacology.<sup>2,22,23,25,28,29</sup> The discrepancies appear to be related to differences in the cellular systems and the types of assays used. For example, cannabidiol (CBD) acts as a GPR55 antagonist preventing agonist-effect in [<sup>35</sup>S]GTPγS, Rho activation,<sup>7,18,20</sup> and is inactive in intracellular Ca<sup>2+</sup> mobilization<sup>30</sup> and β-arrestin recruitment assays.<sup>29</sup>

Growing interest in GPR55 validation as a therapeutic target has focused research in the identification of new, selective synthetic GPR55 ligands. In this context, high-throughput screening of compounds from Molecular Libraries Probe Production Centers Network (MLPCN) using β-arrestin assays has identified different GPR55 chemical scaffolds.<sup>31,32</sup> The triazoloquinoline CID1172084 and the thienopyrimidine CID1434953, discovered in this study and whose structures are represented in Figure 1, exemplify the cases of potent GPR55 agonists and GPR55 antagonists respectively. Parallel studies developed by GlaxoSmithKline validated benzylpiperazines as GPR55 agonists in *Saccharomyces cerevisiae* yeast and in HEK293 cells (e.g., GSK494581A (Figure 1)).<sup>33</sup> Recently, Kargl and coworkers<sup>34</sup> confirmed the GPR55 antagonism of CID16020046 (Figure 1), originated from the MLSCN screening, in yeast cells and HEK293 cells stably expressing GPR55. A β<sub>2</sub>-adrenergic agonist, MNF (Figure 1) was recently described as a selective antagonist of GPR55 signaling as shown through different biological readouts such as ERK phosphorylation and cell motility.<sup>35</sup>

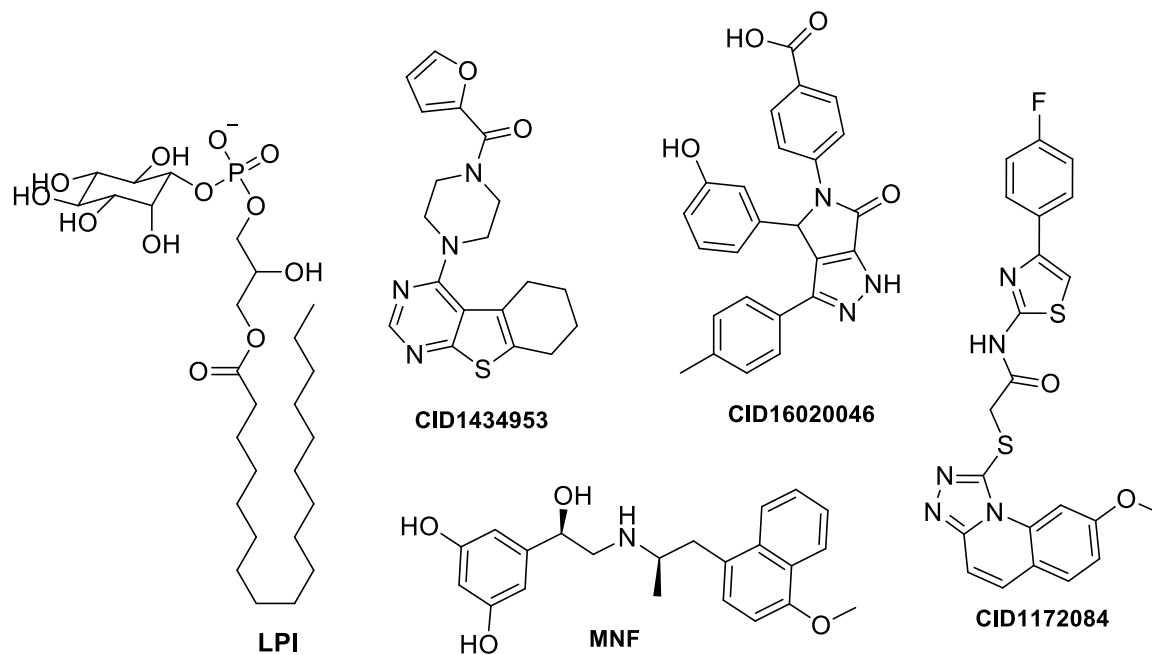


**Figure 1.** Chemical structures of GPR55 ligands.

Exploration of the orphan receptor GPR55 has proven to be problematic mainly due to the lack of GPR55 ligand specificity and selectivity vs classic cannabinoid receptors. Consequently, it becomes crucial to focus our efforts in the discovery of novel potent and selective GPR55 binding molecules that may enable the development of adequate research tools. In this context, and following with the exploration of the chromenopyrazole scaffold previously described by our laboratory,<sup>36–38</sup> the design and synthesis of two different series of GPR55 ligands are presented herein (Figure 2). The design takes into account structural features and inverted-L or T shapes of GPR55 ligands that were suggested in molecular modeling studies published by Reggio and co-workers.<sup>39–41</sup> These studies considered that the binding site of GPR55 active state and inactive state may accommodate inverted-L, 7 or T shaped ligands exposing their most electronegative region in the head part (agonists) or close to the far end of the central section (antagonists).

While CB<sub>1</sub>R and CB<sub>2</sub>R couple to G-proteins of the G<sub>i/o</sub> subfamily, as widely demonstrated in the literature,<sup>42,43</sup> GPR55 has been associated with different G-proteins such as G<sub>α13</sub>,<sup>23</sup> G<sub>αq/11</sub>,<sup>44</sup> G<sub>αq</sub>/G<sub>α12</sub> or G<sub>α12/13</sub>.<sup>23</sup> This G-protein coupling promiscuity depends on the specific GPR55 ligand used and the type of cell line. By engaging these G proteins, GPR55 activates a range of signaling pathways, including RhoA, MAPK cascades, actin filament formation or intracellular calcium release via the activity of phospholipase C (PLC). GPR55 properties have been intensely explored through different functional endpoint assays such as GTPγS binding,<sup>7</sup> analysis of intracellular calcium levels,<sup>23,30</sup> phosphorylation of ERK1/2,<sup>25,26</sup> and the activation of the small GTPase proteins Rac1, RhoA and Cdc42.<sup>7,23,30</sup> GPR55 can also interact with β-arrestin, offering yet another potential cell signaling route.<sup>29</sup> In the present study, the GPR55 activity of the new compounds was assessed using a label-free methodology based on cellular impedance measurements in real time (xCELLigence, ACEA Biosciences). Measuring the whole-cellular integrated response overcomes discrepancies occurring for pharmacological GPR55 ligand characterization related to different pathways. This technology has been widely used for cell viability, proliferation, cytotoxicity, adhesion, invasion, and migration.<sup>45</sup> Recent studies have validated this impedance-based technology for monitoring GPCR activation and signaling in cells.<sup>46–48</sup> Label free technology has been successfully used to assay GPR55 ligands in previous work employing dynamic mass redistribution technology.<sup>49</sup> However, this is the first time that label free cellular impedance measurements are used to screen GPR55 ligands. xCELLigence methodology has been validated with LPI species in stably expressing GPR55-HEK293 cells and human osteoclasts.<sup>50,51</sup>

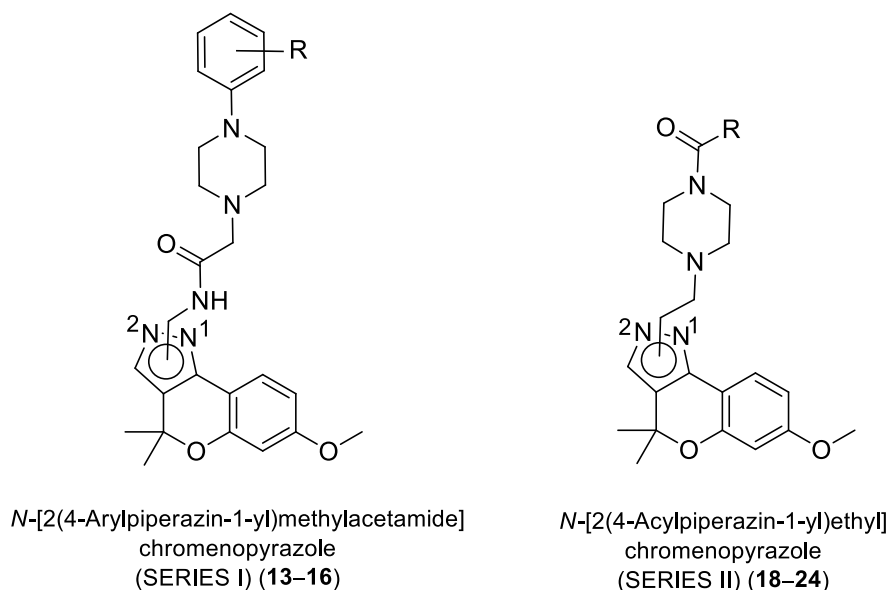


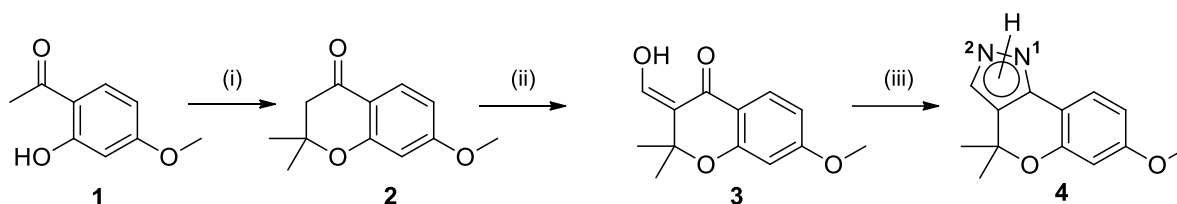
**Figure 2.** Proposed general structures for potential GPR55 activity.

## RESULTS AND DISCUSSION

Studies realized by Reggio and co-workers<sup>39,41</sup> suggested that GPR55 ligands adopt an inverted-L, 7 or a T shape with the presence of an electronegative region located close to the head region (agonist) or in the central portion of the molecule (antagonist). Conformational analysis of two pyrazole isomers from each series, I and II, performed using *ab initio* Hartree-Fock calculations at the 6-31G\* level, and their corresponding electrostatic potential density surfaces using Spartan '08 (See Supporting Information for details) allow us to consider the chromenopyrazole as an interesting scaffold for GPR55 activity. In a first approximation and in comparison with Reggio's data,<sup>39,41</sup> the new compounds adopted inverted-L shape for both series and the localization of their highest electronegative area suggest agonism for series I and antagonism for series II.

**Chemistry.** The chromenopyrazole core (**4**) of the new compounds was prepared following the synthetic route depicted in Scheme 1. 7-Methoxy-2,2-dimethyl-2,3-dihydrochromen-4-one (**2**)

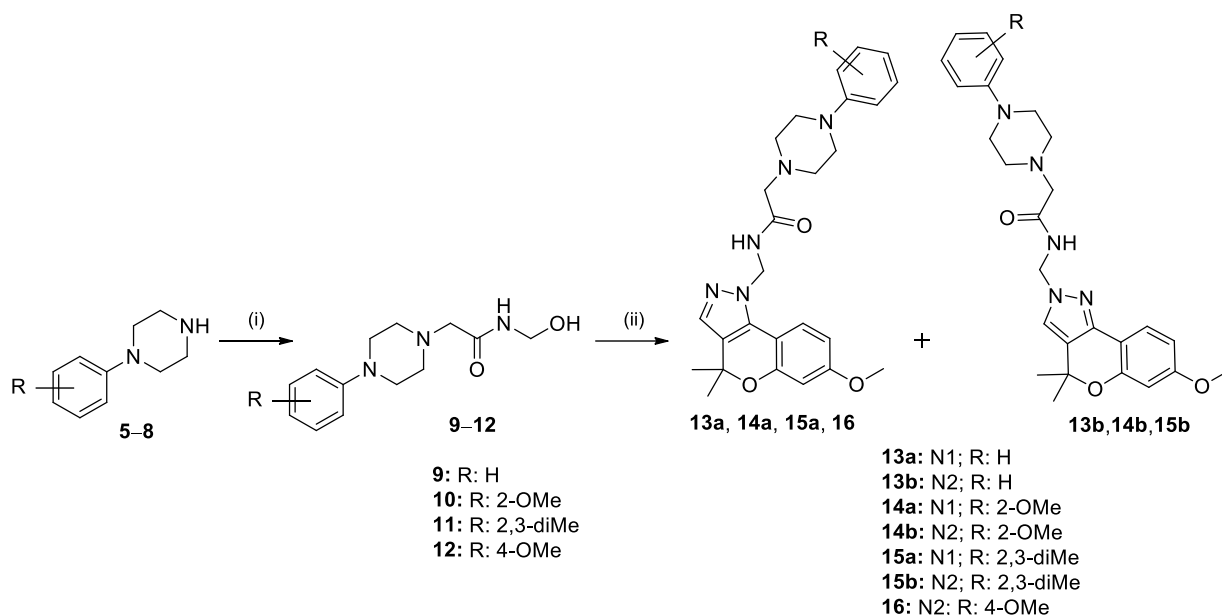
was obtained by cyclization of the commercially available 2-hydroxy-4-methoxyacetophenone (**1**) with acetone.<sup>52–54</sup>  $\alpha$ -Formylation of **2** was achieved under microwave irradiation<sup>36</sup> conditions to result in 3-hydroxymethylenechromen-4-one (**3**).<sup>54</sup> Finally, condensation of the  $\beta$ -keto aldehyde with anhydrous hydrazine<sup>36</sup> yielded 7-methoxy-4,4-dimethyl-1,4-dihydrochromeno[4,3-*c*]pyrazole (**4**) in good yield.<sup>55</sup>



**Scheme 1.** Synthesis of 7-methoxy-4,4-dimethyl-1,4-dihydrochromeno[4,3-*c*]pyrazole (**4**). Reaction conditions: (i) Acetone, pyrrolidine, EtOH, 5 h, reflux, 82%; (ii) NaH, THF, MW, 45 °C, 25 min, then ethyl formate, THF, MW, 45 °C, 25 min, 52%; (iii) Anhydrous hydrazine, EtOH, 2 h, 60 °C, 69%.

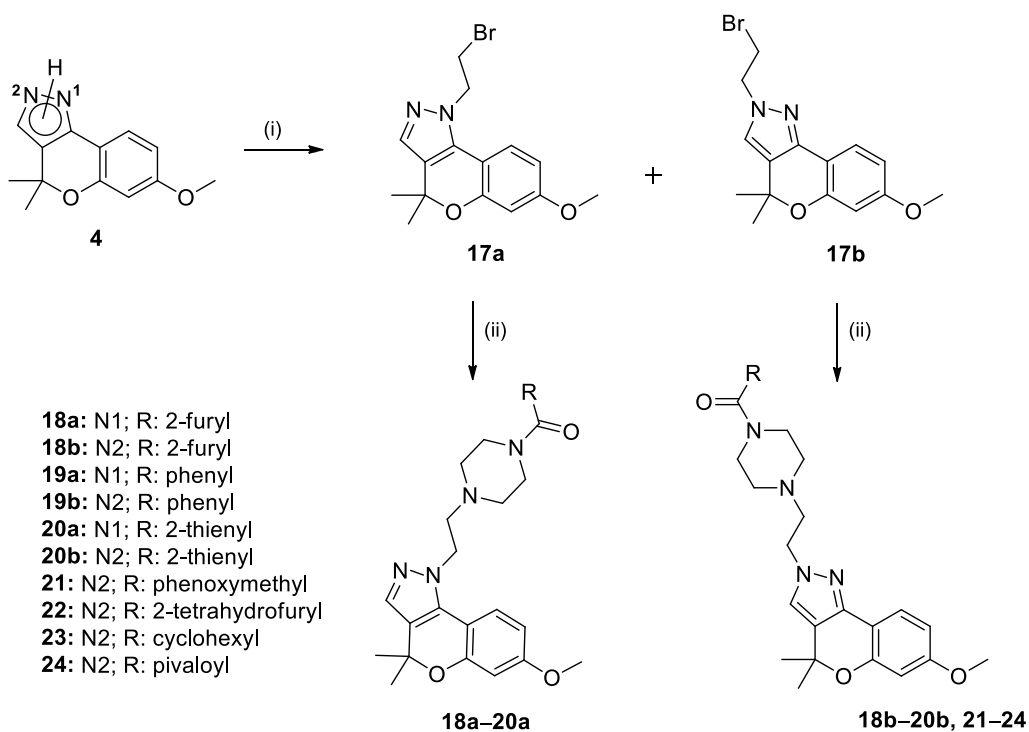
The route depicted in Scheme 2 was used for the preparation of compounds of series I. Arylpiperazines **5–8** were first synthesized by *N*-alkylation of the suitable phenylpiperazine with 2-chloro-*N*-hydroxymethylacetamide to give the piperazines **9–12**. Then, the final compounds **13–16** were prepared by alkylation of 7-methoxy-1,4-dihydro-4,4-dimethylchromeno[4,3-*c*]pyrazole (**4**) with the corresponding phenylpiperazine derivative **5–8** under refluxing conditions. Purification of the *N*1 and *N*2 regioisomers was difficult, in most cases obtaining the desired compounds with low yields. Flash column chromatography followed by a semipreparative HPLC was required to separate both phenylpiperazinyl-acetamidomethyl chromenopyrazoles isomers (**13a–15a** and **13b–15b**).





**Scheme 2.** Synthesis of chromenopyrazoles of serie I (**13–16**). Reaction conditions: **(i)** 2-Chloro-*N*-hydroxymethylacetamide,  $K_2CO_3$ , acetonitrile, 2–5 h, reflux (24–63%); **(ii)** Compound **4**, NaH, THF, 12–72 h, reflux (2–14%).

Acyl-piperazinyl chromenopyrazoles of series II (**18–24**) were obtained starting from chromenopyrazole **4**, as shown in Scheme 3. Alkylation of **4** with 1,2-dibromoethane afforded the desired 2-bromoethylchromenopyrazoles **17a** and **17b**. Both regioisomers were easily separated by medium pressure column chromatography. Finally, compounds **18–24** were obtained reacting the corresponding 2-bromoethylchromenopyrazole (**17a** or **17b**) with the desired acyl piperazines in regular to good yields under refluxing conditions.



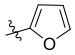
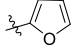
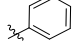
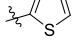
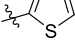
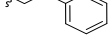
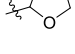
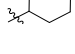

**Scheme 3.** Synthesis of chromenopyrazoles of serie II (**18–24**). Reaction conditions: (i) 1,2-Dibromoethane, NaH, THF, 4 h, reflux, 21 and 40%; (ii) Acyl piperazine, K<sub>2</sub>CO<sub>3</sub>, THF, overnight, reflux, 23-81%.

**Impedance-based cellular assays in hGPR55-HEK293.** As commented in the introduction, the pharmacology of GPR55 is rather puzzling. Moreover, the paucity of structural data and selective potent modulators has also limited the development of accurate pharmacological assays such as radioligand binding assays. In fact, activity of GPR55 ligands is completely influenced by the assay used to assess receptor mediated downstream signaling. Therefore, it was important to use a pharmacological assay able to integrate the different GPR55 signaling pathways. Thus, the potential GPR55 activity of the new chromenopyrazole derivatives was assessed using xCELLigence experiments.<sup>56</sup> The xCELLigence assay detects cellular morphological changes triggered by ligand-dependent GPCR activation and coupling to downstream pathways. These

changes modulate the physical contact between cell and electrode which is reflected by changes in electrical impedance (converted to cell index units by the system). Therefore, measuring the whole-cellular integrated response overcomes discrepancies occurring for pharmacological GPR55 ligand characterization related to different pathways.

Cellular impedance of increasing concentrations of LPI and chromenopyrazoles **13–16** and **18–24** was monitored in a human embryonic kidney 293 cell line stably overexpressing recombinant human GPR55 (hGPR55-HEK293). Cells were seeded one day prior to stimulation with the compounds to ensure attachment to the microelectrodes located in the bottom of the culture plate. Activation of the receptor by a GPR55 ligand causes changes in cellular impedance detected in real time by the xCELLigence system. Agonistic effects of tested compounds were compared to the activity of GPR55 agonist LPI (LPI effect at 1  $\mu$ M is set at 100%). Dose-response curves were obtained plotting the peak cell index response (five minutes after administration of the drugs), versus the logarithm of the concentration for each compound. Cell index values were normalized for each well to the time point immediately preceding agonist addition. Half maximal effective concentration values ( $EC_{50}$ ) and the corresponding maximal effect ( $E_{max}$ ) of LPI and chromenopyrazole derivatives are displayed in Table 1. The activity observed for LPI was consistent with published data in all the experiments.<sup>57</sup>

**Table 1.** Agonism of chromenopyrazole derivatives **13–16** and **18–24** at GPR55 receptor measured using xCELLigence system.

Compd	R	Subst.	GPR55	
			EC <sub>50</sub> (nM) <sup>a</sup>	E <sub>max</sub> (%) <sup>b</sup>
<b>13a</b>	H	N1	-	NR
<b>13b</b>	H	N2	-	NR
<b>14b</b>	2-OMe	N2	6.36 (0.98-41.52)	51 (36-67)
<b>15b</b>	2,3-diMe	N2	-	NR
<b>16</b>	4-OMe	N1	-	NR
<b>18a</b>		N1	-	NR
<b>18b</b>		N2	0.88 (0.05-14.56)	43 (31-54)
<b>19b</b>		N2	0.60 (0.12-3.03)	51 (42-60)
<b>20a</b>		N1	-	NR
<b>20b</b>		N2	0.51 (0.06-4.22)	45 (36-54)
<b>21</b>		N2	1.28 (0.20-9.46)	52 (41-63)
<b>22</b>		N2	0.40 (0.03-4.61)	51 (40-62)
<b>23</b>		N2	8.67 (1.18-63.45)	47 (36-58)
<b>24</b>		N2	0.69 (0.06-7.63)	49 (37-62)
LPI	-	-	2.82 (0.64-12.30)	100 (81-118)

The data is presented as a percentage of the maximal LPI stimulation (at 1  $\mu$ M, LPI displays off-target activity at 10  $\mu$ M). <sup>a</sup>EC<sub>50</sub> values were calculated using nonlinear regression analysis. Data represent the mean of at least four experiments performed in duplicate, and 95% confidence intervals (CI) for the EC<sub>50</sub> values are given in parentheses. <sup>b</sup>E<sub>max</sub>: Maximal agonist effect, determined using nonlinear regression analysis (95% CI). NR: No response at tested concentrations (E<sub>max</sub> lower than 25% relative to LPI). Subst.: substitution.

According to the ability to activate GPR55, there is a clear difference between both series of compounds (**13–16** and **18–24**). All tested chromenopyrazoles of series II exhibited agonistic GPR55 profile except **18a** and **20a**. Conversely, chromenopyrazoles of series I did not have capacity to activate GPR55 in this cell model, excluding **14b**, which partially activated the receptor. Compared to the LPI response, active compounds (**14b**, **18b**, **19b**, **15b**, **20b**, and **21–24**) displayed partial agonism in GPR55-HEK293 cells exhibiting good potency with  $EC_{50}$  values in the nanomolar range. However, they displayed half of the maximal efficacy of the putative endogenous modulator LPI. Concentration-response curves of LPI and compounds **14b** and **21** are displayed in Figure 3 to exemplify the GPR55 agonism effect (Concentration-response curves of **18b**, **19b**, **20b**, **22–24** are reported in the Supporting Information).

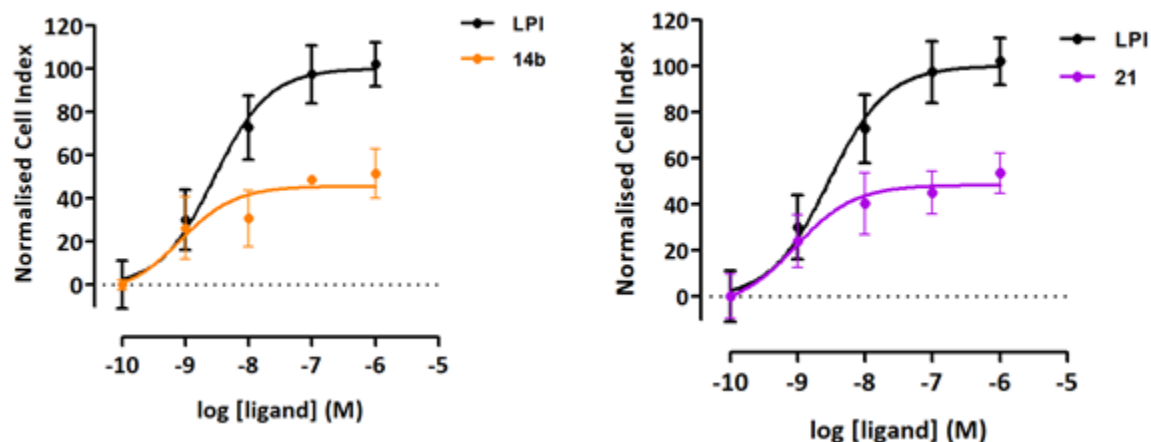


**Figure 3.** Concentration-response curves of LPI and representative chromenopyrazole derivatives **14b** and **21** in hGPR55-HEK293 cells using xCELLigence system. Data points represent the mean  $\pm$  SEM values of four independent experiments, performed in duplicate. The data is presented as a percentage of the maximal LPI stimulation (at 1  $\mu$ M, LPI displays off-target activity at 10  $\mu$ M).

Interestingly, in series II, the *N*1- or *N*2-chromenopyrazole substitution influenced the ability of the compounds to activate GPR55. *N*2-regioisomers (**18b**, **19b**, **20b**, **21** and **24**) is the preferred substitution while substitution at *N*1-position (**18a** and **20a**) exerted a negative impact on GPR55 activation. Figure 4 illustrates the effects of both isomers taking as examples *N*1- (**18a**) and *N*2-substituted (**18b**), on dose-response curves in hGPR55-HEK293 cells.

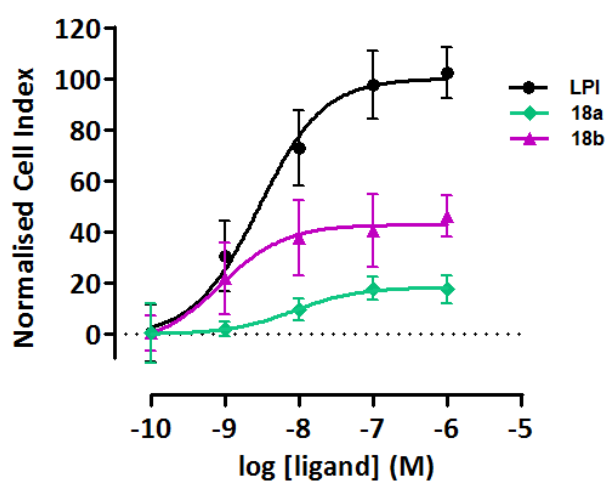
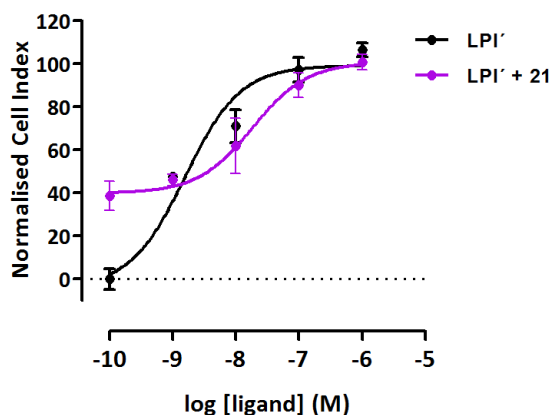


**Figure 4.** Concentration-response curves of LPI and representative chromenopyrazole derivatives **18a** and **18b** in hGPR55-HEK293 cells using xCELLigence system. Data points represent the mean  $\pm$  SEM values of four independent experiments, performed in duplicate. The data is presented as a percentage of the maximal LPI stimulation (at 1  $\mu$ M, LPI displays off-target activity at 10  $\mu$ M).

After analyzing the ability of the compounds to activate GPR55, their potential antagonistic activity was evaluated. The capacity of **13–16** and **18–24** to inhibit LPI-mediated GPR55 stimulation was assessed at 1  $\mu$ M. Full concentration-response curves for LPI in presence and absence of all new synthesized compounds were determined (Table 2). Graphs displayed in Figure 5 exemplify the antagonism effect taking as example compound **21** (Concentration-

response curves of LPI in presence of **22–24** are reported in the Supporting Information). These experiments were performed by co-incubation of the cells with the tested compounds (or vehicle) and different concentrations of the standard agonist LPI.

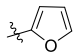
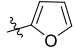
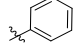
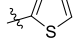
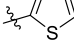
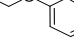
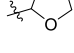
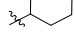

As shown in Table 2, many of the chromenopyrazoles of series II were able to inhibit LPI dose-dependent GPR55 activation. Among them, **21**, **22**, **23** and **24** exerted significant capacity to antagonize LPI effect at 1  $\mu$ M. As previously demonstrated, these compounds are also partial agonists of the receptor when administered alone.



**Figure 5.** Concentration-response curves of LPI in the presence and absence of chromenopyrazoles **21** in hGPR55-HEK293 cells using xCELLigence system. Data points represent the mean  $\pm$  SEM values of at least four independent experiments, performed in duplicate. The data is presented as a percentage of the maximal LPI stimulation.

**Table 2.** Potencies and maximal effect of LPI in the presence and absence of chromenopyrazoles **13–16** and **18–24** (1  $\mu$ M) at GPR55.

Compd	R	Subst.	GPR55
-------	---	--------	-------

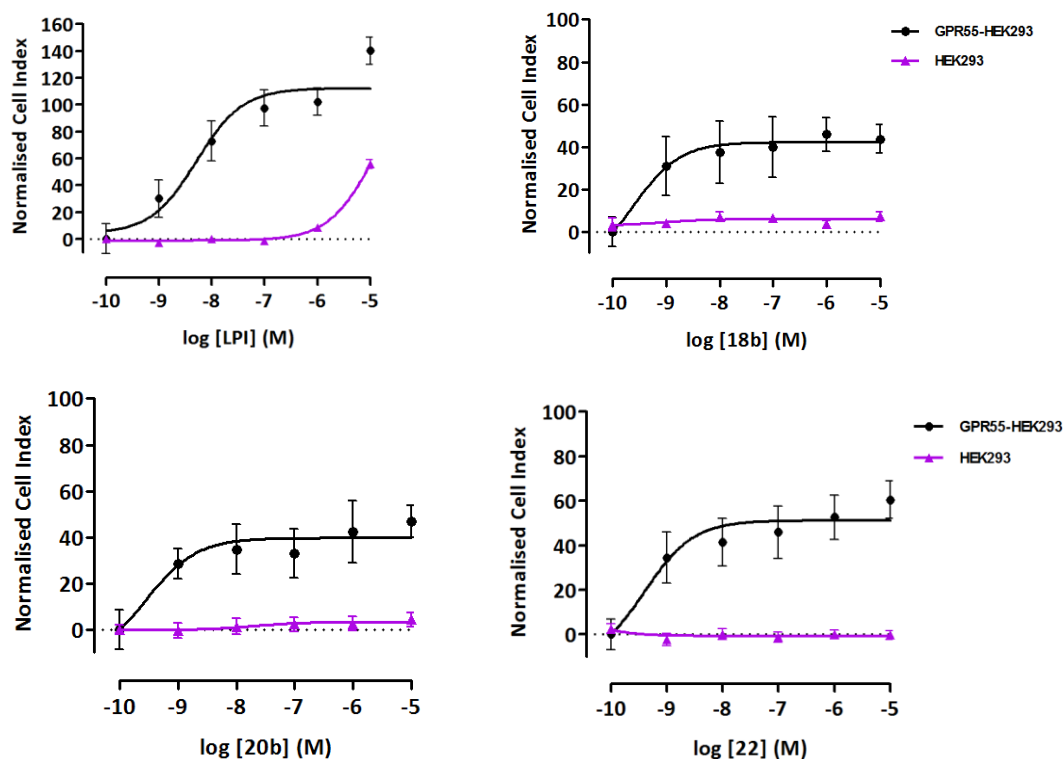
			EC <sub>50</sub> (nM) <sup>a</sup>	E <sub>max</sub> (%) <sup>b</sup>
LPI + <b>13a</b>	H	N1	27.7 (8.9-86.1)	97 (80-115)
LPI + <b>13b</b>	H	N2	31.5 (5.4-83.6)	94 (78-108)
LPI + <b>14b</b>	2-OMe	N2	28.4 (4.7-96.1)	90 (71-104)
LPI + <b>15b</b>	2,3-diMe	N2	30.4 (10.1-91.5)	102 (90-115)
LPI + <b>16</b>	4-OMe	N1	27.3 (1.2-97.5)	80 (60-105)
LPI + <b>18a</b>		N1	19.6 (5.9-65.3)	97 (83-111)
LPI' + <b>18b</b>		N2	19.8 (3.9-76.1)	106 (92-120)
LPI' + <b>19b</b>		N2	15.5 (3.8-54.6)	105 (96-113)
LPI + <b>20a</b>		N1	29.3 (8.4-79.2)	99 (82-116)
LPI' + <b>20b</b>		N2	8.2 (2.5-26.4)	96 (87-106)
LPI' + <b>21*</b>		N2	18.2 (4.6-71.1)	100 (91-115)
LPI' + <b>22*</b>		N2	24.6 (7.9-66.8)	102 (91-106)
LPI' + <b>23*</b>		N2	25.4 (6.6-96.7)	99 (90-113)
LPI' + <b>24*</b>		N2	21.9 (5.5-87.6)	100 (86-114)
LPI	-	-	4.1 (1.3-12.1)	104 (91-114)
LPI'	-	-	1.6 (0.6-4.2)	99 (90-108)

<sup>a</sup>EC<sub>50</sub> values were calculated using nonlinear regression analysis. Data represent the mean of at least four experiments performed in duplicate, and 95% confidence intervals (CI) for the EC<sub>50</sub> values are given in parentheses. <sup>b</sup>E<sub>max</sub>: Maximal agonist effect, determined using nonlinear regression analysis (95% CI). \*Significantly different (non-overlapping confidence intervals) from the corresponding LPI alone. The effect of each compound over LPI dose-response is related to their corresponding LPI (LPI or LPI') in absence of the potential antagonist. Subst.: substitution.



Taking into consideration the xCELLigence impedance assays presented in this study, the most promising results come from series II. Three (acylpiperazinyl)ethyl chromenopyrazoles (**18b**, **19** and **20b**) displayed capacity to partially activate GPR55, while **21–24** displayed both partial agonism and antagonism of LPI response. From series I, only one compound (**14b**) showed GPR55 partial agonism.

**Impedance-based cellular assays in normal HEK293.** The assays described above were performed in hGPR55-HEK293 cells, thus, the observed effects are suggestive of a mechanism mediated through GPR55. However, this hypothesis needs to be verified since this technology measures integrative cell response. To confirm that the observed agonism and antagonist effects are actually mediated by GPR55, compounds were evaluated in normal HEK293 cells. Full dose-response curves of all the new compounds and LPI were performed at concentrations from 1 nM to 10  $\mu$ M in normal HEK293 cells. Chromenopyrazoles **13–16** and **18–24** did not exhibit any response at doses up to 10  $\mu$ M in normal cells which highlights that the effects observed in HEK293 cells overexpressing GPR55 are mediated through GPR55. It is worthy to note that LPI clearly displayed off-target stimulation at high concentrations (10  $\mu$ M). These off-target effects of LPI at doses over 10  $\mu$ M had already been reported through diverse functional endpoints.<sup>58,59</sup> To exemplify the lack of effect in HEK293 cells compared to GPR55-HEK293 cells, graphs of three new GPR55 agonists (**18b**, **20b**, and **22**) and LPI are shown in Figure 6 comparing their effect in GPR55 transfected and normal HEK293 cells.

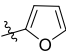
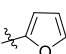
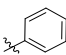
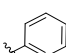
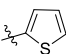
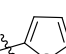
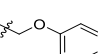


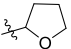
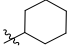

**Figure 6.** Concentration-response curves of LPI and **18b**, **20b**, and **22** in hGPR55-HEK293 and normal HEK293 cells. Data points represent the mean  $\pm$  SEM values of four independent experiments, performed in duplicate. The data are presented as a percentage of the maximal LPI stimulation.

**CB<sub>1</sub>R and CB<sub>2</sub>R binding assays.** Most of the GPR55 ligands identified so far are also able to interact with CBRs. In order to further investigate the selectivity of the new compounds *vs* classical cannabinoid receptors, their capacity to bind to CB<sub>1</sub>R and CB<sub>2</sub>R was evaluated. The affinities of compounds **13–16** and **18–24** were determined by radioligand binding studies at human CB<sub>1</sub>R (hCB<sub>1</sub>R) and human CB<sub>2</sub>R (hCB<sub>2</sub>R) using [<sup>3</sup>H]CP55940 as radioligand. As a source for hCB<sub>1</sub>R and hCB<sub>2</sub>R, membrane preparations of HEK293 EBNA cells stably expressing the respective receptor type were used. Initially, compounds were screened at 40  $\mu$ M. In those

cases in which the inhibition of radioligand binding was at least about 70%, competition curves using a broad range of compound concentrations were performed in order to calculate  $K_i$  values. The experimental binding affinities of **13–16**, **18–24** and for the reference cannabinoid WIN55,212-2 are reported in Table 3.

**Table 3.** Binding affinity of compounds **13–16** and **18–24** and the reference cannabinoid WIN55,212-2 for hCB<sub>1</sub> and hCB<sub>2</sub> cannabinoid receptors.

Compd	R	Subst.	CB <sub>1</sub> R and CB <sub>2</sub> R	
			hCB <sub>1</sub> $K_i$ (nM) <sup>a</sup>	hCB <sub>2</sub> $K_i$ (nM) <sup>a</sup>
<b>13a</b>	H	N1	>40000	4923 ± 349
<b>13b</b>	H	N2	>40000	1578 ± 461
<b>14a</b>	2-OMe	N1	>40000	>40000
<b>14b</b>	2-OMe	N2	>40000	>40000
<b>15a</b>	2,3-diMe	N1	>40000	>40000
<b>15b</b>	2,3-diMe	N2	>40000	>40000
<b>16</b>	4-OMe	N1	>40000	>40000
<b>18a</b>		N1	>40000	nd
<b>18b</b>		N2	>40000	698 ± 107
<b>19a</b>		N1	>40000	nd
<b>19b</b>		N2	>40000	3604 ± 941
<b>20a</b>		N1	>40000	nd
<b>20b</b>		N2	>40000	15.4 ± 7.8
<b>21</b>		N2	>40000	>40000

<b>22</b>		N2	>40000	1073 ± 238
<b>23</b>		N2	>40000	523 ± 144
<b>24</b>		N2	>40000	6392 ± 327
WIN55,212-2	-	-	45.6 ± 8.6	3.7 ± 0.2

<sup>a</sup>Values obtained from competition curves using [<sup>3</sup>H]CP55940 as radioligand for hCB<sub>1</sub>R and hCB<sub>2</sub>R cannabinoid receptors and are expressed as the mean ± SEM of at least three experiments. nd: not determined.

Tested compounds from both series showed no affinity towards CB<sub>1</sub>R. Thus, they are all devoid of psychotropic side-effects associated with the activation of CB<sub>1</sub>R in the brain. From series I, chromenopyrazoles **14–16** did not bind to CB<sub>2</sub>R. However, when the phenyl group is not substituted (**13a** and **13b**), a moderate CB<sub>2</sub>R affinity was displayed. From this series, compound **14b**, which showed to be GPR55 partial agonist, stands out due to its selectivity for GPR55 vs CB<sub>1</sub>R and CB<sub>2</sub>R.

Regarding series II, compound **21** lacked of affinity for both receptors whereas compounds **24** and **19b** showed low affinity for CB<sub>2</sub>R. Considering the GPR55 partial agonist/LPI antagonist properties of **21** and its GPR55 selectivity vs CB<sub>1</sub>R and CB<sub>2</sub>R, chromenopyrazole **21** appears to be a good lead compound for further development. This molecule bears a phenoxyacetyl piperazine which is the largest substituent assessed within this series. This fact may indicate that smaller substituents are preferred for CB<sub>2</sub>R binding.

From this series, **18b**, **20b**, **22**, and **23** revealed moderate to high affinity towards CB<sub>2</sub>R. Since the CB<sub>2</sub>R affinity constant of **20b** was in the nanomolar range, the functionality at this receptor has been determined by GTP-γ assay. Thus, compound **20b** was shown to be potent CB<sub>2</sub>R agonist (EC<sub>50</sub>: 391.5 ± 125.9 nM; E<sub>max</sub>: 87.8 ± 7.5%). Even though our main purpose is the

identification of GPR55 selective ligands, a dual GPR55-CB<sub>2</sub> drug may open novel therapeutic strategies due to the close relation of both GPCRs in different pathologies.<sup>60,61</sup>

**In silico ADME properties.** So far, the most potent known ligand for GPR55 is LPI. However, LPI is very insoluble in water, and it is unstable when exposed to air or light; it oxidizes very easily. Due to these particularities, LPI is not suitable as therapeutic agent. Therefore, ADME properties of **13–16**, **18–24** and LPI was predicted using a set of 34 physicochemical descriptors computed by QikProp. The predicted parameters (Supporting Information) suggest a clear ADME improvement compared to LPI.

## CONCLUSION

The first selective GPR55 ligands were discovered only a few years ago. Since then, few new structures have been reported due to the lack of binding assays and discrepancies of different functional outcomes. In this context the design adopted in this study, and based on shape features of previously investigated GPR55 ligands, allowed the discovery of a novel GPR55 scaffold. Synthesis and pharmacological activity of two series of chromenopyrazoles as GPR55 ligands is reported herein. The pharmacological evaluation was accomplished in a cell-impedance based assay that allows taking into account the complex signaling pathways related to GPR55 activation. This label-free technology approach is adding value to the drug discovery process taking into account the lack of available GPR55 radioligand. These functional assays revealed **14b** from series I as a partial agonist with full GPR55 selectivity vs classic CBRs. Excluding the *N*1-substituted pyrazoles **18a** and **20a**, all chromenopyrazoles of series II showed GPR55-mediated effects. However, compared to LPI efficacy they are partial agonist of GPR55 (**18b**, **19** and **20b**). Four of them (**21–24**) displayed both GPR55 partial agonism and antagonism of LPI

response. Moreover, chromenopyrazole **21** bearing a phenoxyethyl substituent is devoid of any CBR activity. SARs clearly highlight the *N2*-preferred chromenopyrazole substitution in both series. It is noteworthy that the new compounds did not show any effect on normal HEK293 cells confirming that the effects in GPR55-HEK293 cells were mediated through GPR55. Although LPI possesses good activity and can activate GPR55 using different functional readouts, it is still prone to important disadvantages such as poor solubility and stability. In this scenario, the chromenopyrazoles **14b** and **21** with improved predicted ADME are potential candidates to generate helpful pharmacological tools or potential drugs for novel therapeutic strategies.

## EXPERIMENTAL SECTION

### **Chemistry.**

*General methods and materials.* Reagents and solvents were purchased from Sigma-Aldrich Co., Fluorochem, Acros Organics, Manchester Organics and Lab-Scan and were used without further purification or drying. Microwave assisted organic synthesis was performed using the microwave reactor Biotage Initiator. Products were purified using flash column chromatography (Merck Silica gel 60, 230-400 mesh) or medium pressure chromatography using Biotage Isolera One with pre-packed silica gel columns (Biotage SNAP cartridges). Semipreparative HPLC purifications were performed on a Waters 2695 HPLC system equipped with a Photodiode Array 2998 coupled to a 3100 Mass Detector mass spectrometer, using a Sunfire C18 column (19 mm x 150 mm) and 70 min gradient A: CH<sub>3</sub>CN/0.1% formic acid, B: H<sub>2</sub>O/0.1% formic acid monitoring at  $\lambda = 254$  nm. The flow rate was 24 mL/min. The compounds were characterized by a combination of NMR experiments, HPLC-MS, high resolution mass spectrometry (HRMS) and elemental analysis. Analytical HPLC-MS analysis was performed on a Waters 2695 HPLC

system equipped with a photodiode array 2996 coupled to Micromass ZQ 2000 mass spectrometer (ESI-MS), using a reverse-phase column SunFire™ (C-18, 4.6 x 50 mm, 3.5 μm) and 10 min gradient A: CH<sub>3</sub>CN/0.1% formic acid, B: H<sub>2</sub>O/0.1% formic acid visualizing at λ = 254 nm. Flow rate was 1 mL/min. Elemental analyses of the compounds were performed using a LECO CHNS-932 apparatus. Deviations of the elemental analysis results from the calculated are within ± 0.4%. The purity of compounds was determined by LC coupled to high resolution mass spectrometry. The purity of all tested compounds was higher than 95%. The experiments were performed in a LC-MS hybrid quadrupole/time of flight (QTOF) analyzer equipped with an Agilent 1100 LC coupled to an Agilent 6500 Accurate Mass (1-2 ppm mass accuracy) using electrospray ionization in the positive mode (ESI<sup>+</sup>). <sup>1</sup>H, <sup>13</sup>C, HSQC and HMBC-NMR spectra were recorded on a Mercury 400 (400 and 101 MHz) or a Varian 500 (500 and 126 MHz) at 25 °C. Samples were prepared as solutions in deuterated solvent and referenced to internal non-deuterated solvent peak. Chemical shifts were expressed in ppm (δ) downfield of tetramethylsilane. Coupling constants are given in hertz (Hz). Melting points were measured on a MP 70 Mettler Toledo apparatus.

The preparation procedure, structural characterization, and purity of intermediates **2-4** are reported in the Supporting Information.

**General procedure for the synthesis of phenylpiperazinylacetamides 9-12.** To a mixture of the corresponding phenylpiperazine (1 eq) and K<sub>2</sub>CO<sub>3</sub> (1.5 eq) in acetonitrile, a solution of 2-chloro-*N*-hydroxymethylacetamide (2 eq) in acetonitrile was added. The reaction was refluxed for 2-5 h. After reaction completion, the solvent was removed under reduced pressure. The resultant crude was diluted by EtOAc, washed with water and extracted three times with EtOAc. The combined organic layers were dried over MgSO<sub>4</sub>, filtered and the solvent was evaporated

under vacuum. The residue was purified by flash column chromatography performed on a Biotage Isolera One. The chromatography eluent and yield are indicated below for each reaction.

***N*-Hydroxymethyl-2-(4-phenylpiperazinyl)acetamide (9).** Flash column chromatography (EtOAc) gave **9** as a white solid (0.42 g, 41% yield); mp: 112-114°C; <sup>1</sup>H-NMR (400 MHz, CDCl<sub>3</sub>) δ: 8.10-8.02 (br s, 1H, NH), 7.39-7.22 (m, 2H, phenyl), 7.06-6.85 (m, 3H, phenyl), 4.82 (s, 2H, CH<sub>2</sub>OH), 3.28-3.19 (m, 4H, piperazine), 3.13 (s, 2H, COCH<sub>2</sub>), 2.90-2.57 ppm (m, 4H, piperazine); <sup>13</sup>C-NMR (101 MHz, CDCl<sub>3</sub>) δ: 173.6 (CO), 151.5 (C<sub>Ph</sub>-N), 129.8, 129.7, 120.5, 119.3 and 116.7 (C<sub>Ph</sub>), 73.1(CH<sub>2</sub>OH), 62.0 (COCH<sub>2</sub>), 54.1, 53.7, 50.9 and 49.8 ppm (piperazine); HPLC-MS: [A, 2% →95%], t<sub>R</sub>: 2.46 min (93%), MS (ES<sup>+</sup>, m/z) 250 [M+H]<sup>+</sup>; Anal. Calcd. for C<sub>13</sub>H<sub>19</sub>N<sub>3</sub>O<sub>2</sub>: C 62.63%, H 7.68%, found: C 62.41%, H 7.83%.

***N*-Hydroxymethyl-2-[4-(2-methoxyphenyl)piperazinyl]acetamide (10).** Flash column chromatography (EtOAc) afforded **10** as a white solid (1.06 g, 63% yield); mp: 134-136 °C; <sup>1</sup>H-NMR (400 MHz, CDCl<sub>3</sub>) δ: 8.14-8.11 (br s, 1H, NH), 7.03-6.96 (m, 2H, phenyl), 6.89- 6.78 (m, 2H, phenyl), 4.79 (s, 2H, CH<sub>2</sub>OH), 3.94-3.64 (m, 5H, COCH<sub>2</sub> and OCH<sub>3</sub>), 3.17-2.89 (m, 4H, piperazine), 2.84-2.66 ppm (m, 4H, piperazine); <sup>13</sup>C-NMR (101 MHz, CDCl<sub>3</sub>) δ: 171.4 (CO), 151.7 (C<sub>Ph</sub>-N), 140.4 (C<sub>Ph</sub>- OCH<sub>3</sub>), 122.6, 120.5, 117.6 and 110.8 (C<sub>Ph</sub>), 63.0 (CH<sub>2</sub>OH), 61.0 (COCH<sub>2</sub>), 54.8 (OCH<sub>3</sub>), 53.6, 53.2, 51.0 and 50.1 ppm (piperazine); HPLC-MS: [A, 2% →95%], t<sub>R</sub>: 3.24 min (92%), MS (ES<sup>+</sup>, m/z) 280 [M+H]<sup>+</sup>; Anal. Calcd. for C<sub>14</sub>H<sub>21</sub>N<sub>3</sub>O<sub>3</sub>: C 60.20%, H 7.58%, found: C 60.31%, H 7.72%.

**2-[4-(2,3-Dimethylphenyl)piperazinyl]-*N*-hydroxymethylacetamide (11).** Flash column chromatography (EtOAc) yielded **11** as a white solid (0.11 g, 25% yield); mp: 126-127 °C; <sup>1</sup>H-NMR (400 MHz, CDCl<sub>3</sub>) δ: 8.19-8.14 (br s, 1H, NH), 7.07 (t, *J* = 7.6 Hz, 1H, phenyl), 6.98-6.90 (m, 2H, phenyl), 5.59-5.57 (br s, 1H, OH), 4.82 (s, 2H, CH<sub>2</sub>OH), 3.14 (s, 2H, COCH<sub>2</sub>), 2.94-2.92



(m, 4H, piperazine), 2.77-2.73 (m, 4H, piperazine), 2.27 (s, 3H,CH<sub>3</sub>), 2.21 ppm (s, 3H, CH<sub>3</sub>); <sup>13</sup>C-NMR (101 MHz, CDCl<sub>3</sub>) δ: 173.8 (CO), 172.0 (Cphenyl-N), 151.2, 138.0, 131.3, 125.8 and 125.1 (phenyl), 74.6 (CH<sub>2</sub>OH), 67.3 (COCH<sub>2</sub>), 63.7, 61.5, 54.1 and 52.2 (piperazine), 20.6 (CH<sub>3</sub>), 13.9 ppm (CH<sub>3</sub>); HPLC-MS: [A, 2%→95%], *t*<sub>R</sub>: 3.99 min (90%), MS (ES<sup>+</sup>, *m/z*) 278 [M+H]<sup>+</sup>; Anal. Calcd. for C<sub>15</sub>H<sub>23</sub>N<sub>3</sub>O<sub>2</sub>: C 64.96%, H 8.36%, found: C 65.09%, H 8.03%.

***N*-(Hydroxymethyl)-2-[4-(4-methoxyphenyl)piperazinyl]acetamide (12).** Flash column chromatography (EtOAc) provided **12** as a white solid (0.14 g, 24% yield); mp: 140-143 °C; <sup>1</sup>H-NMR (400 MHz, CDCl<sub>3</sub>) δ: 7.09-6.95 (m, 2H, phenyl), 6.71-6.54 (m, 2H, phenyl), 4.83 (s, 2H, CH<sub>2</sub>OH), 3.78-3.60 (m, 5H, COCH<sub>2</sub> and OCH<sub>3</sub>), 3.14-3.05 (m, 4H, piperazine), 2.77-2.71 ppm (m, 4H, piperazine); <sup>13</sup>C-NMR (101 MHz, CDCl<sub>3</sub>) δ: 173.0 (CO), 152.4 (C<sub>Ph</sub>-N), 143.6 (C phenyl-OCH<sub>3</sub>), 123.4, 122.1, 118.6 and 112.3 (4C phenyl), 65.7 (CH<sub>2</sub>OH), 63.2 (COCH<sub>2</sub>), 55.1 (OCH<sub>3</sub>), 54.3, 53.8, 51.8 and 51.2 ppm (piperazine); HPLC-MS: [A, 2%→95%], *t*<sub>R</sub>: 3.03 min (90%), MS (ES<sup>+</sup>, *m/z*) 280 [M+H]<sup>+</sup>; Anal. Calcd. for C<sub>14</sub>H<sub>21</sub>N<sub>3</sub>O<sub>3</sub>: C 60.20%, H 7.58%, found: C 60.56%, H 7.25%.

**General procedure for the synthesis of phenylpiperazinylacetamidomethyl chromenopyrazoles 13-16.** A solution of **4** (1 eq) in anhydrous THF was added dropwise to a precooled suspension of sodium hydride (2.5-3 eq) in anhydrous THF under nitrogen atmosphere. The resulting mixture was stirred for 10 minutes at room temperature. The corresponding phenylpiperazinyl-acetamide (2 eq) was added and the reaction mixture was refluxed at room temperature 12-72 h. The solvent was removed under vacuum and the crude was diluted in EtOAc, washed with water and extracted three times with EtOAc. The combined organic layers were dried over MgSO<sub>4</sub> and the solvent was removed under vacuum. The residue

was first purified by flash column chromatography (EtOAc as eluent) obtaining a mixture of the *N*1 and *N*2 regioisomers which was then purified by semipreparative HPLC.

**1,4-Dihydro-7-methoxy-4,4-dimethyl-1-[2-(4-phenylpiperazinyl)acetamidomethyl]-chromeno[4,3-*c*]pyrazole (13a) and 2,4-dihydro-7-methoxy-4,4-dimethyl-2-[2-(4-phenylpiperazinyl)acetamidomethyl]-chromeno[4,3-*c*]pyrazole (13b).** Compound **13a** was obtained as a white solid (13% yield); mp: 196-198 °C; <sup>1</sup>H-NMR (500 MHz, CDCl<sub>3</sub>) δ: 8.02-7.97 (br t, *J* = 6.3 Hz, 1H, NH), 7.76 (d, *J* = 8.7 Hz, 1H, 9-H), 7.26 (s, 1H, 3-H), 6.85-6.74 (m, 2H, phenyl), 6.55 (dd, *J* = 8.6, 2.6 Hz, 2H, phenyl), 6.53-6.46 (m, 2H, 8-H and phenyl), 6.45 (d, *J* = 2.5 Hz, 1H, 6-H), 5.73 (d, *J* = 6.3 Hz, 2H, CH<sub>2</sub>NH), 3.71 (s, 3H, OCH<sub>3</sub>), 3.13-3.07 (m, 4H, piperazine), 3.03 (s, 2H, COCH<sub>2</sub>), 2.57-2.48 (m, 4H, piperazine), 1.52 (s, 6H, OC(CH<sub>3</sub>)<sub>2</sub>); <sup>13</sup>C-NMR (126 MHz, CDCl<sub>3</sub>) δ: 170.2 (CO), 165.1 (7-C), 161.0 (5a-C), 154.3 (C<sub>a</sub>), 149.2(9b-C), 133.8 (2C phenyl), 132.5 (3-C), 129.1 (9-C), 123.3 (3a-C), 121.4 (2C phenyl), 120.0 (phenyl), 116.2 (9a-C), 107.8 (8-C), 103.85 (6-C), 76.73 (OC(CH<sub>3</sub>)<sub>2</sub>), 61.3 (COCH<sub>2</sub>), 55.3 (OCH<sub>3</sub>), 54.32 (CH<sub>2</sub>NH), 53.4, 49.1 (piperazine), 28.24 ppm (OC(CH<sub>3</sub>)<sub>2</sub>); HPLC-MS: [A, 15%→40%], *t*<sub>R</sub>: 8.01 min (97%), MS (ES<sup>+</sup>, *m/z*) 462 [M+H]<sup>+</sup>; HRMS calcd for C<sub>26</sub>H<sub>31</sub>N<sub>5</sub>O<sub>3</sub>: 461.2426, found: 461.2433. Compound **13b** was obtained as a white gummy solid (10.2 mg, 5% yield); <sup>1</sup>H-NMR (500 MHz, CD<sub>3</sub>OD) δ: 8.44-8.40 (br s, 1H, NH), 7.51 (d, *J* = 8.5, 1H, 9-H), 7.44 (s, 1H, 3-H), 7.15 – 7.04 (m, 2H, phenyl), 6.82 (dd, *J* = 7.4, 1.0 Hz, 2H, phenyl), 6.72 (tt, *J* = 7.4, 1.0 Hz, 1H, phenyl), 6.47 (dd, *J* = 8.5, 2.4 Hz, 1H, 8-H), 6.39 (d, *J* = 2.4 Hz, 1H, 6-H), 5.40 (s, 2H, CH<sub>2</sub>NH), 3.69 (s, 3H, OCH<sub>3</sub>), 3.10-3.07 (m, 4H, piperazine), 3.02 (s, 2H, COCH<sub>2</sub>), 2.55-2.49 (m, 4H, piperazine), 1.46 ppm (s, 6H, OC(CH<sub>3</sub>)<sub>2</sub>); <sup>13</sup>C-NMR (126 MHz, CD<sub>3</sub>OD) δ: 173.7 (CO), 162.7 (7-C), 156.1 (5a-C), 152.7 (phenyl), 144.6 (9b-C), 130.0 (2 phenyl), 126.6 (3-C), 123.9 (9-C), 122.4 (3a-C), 121.1 (2 phenyl), 117.5 (phenyl), 111.5 (9a-C), 108.8 (8-C), 104.2 (6-C), 77.6

(OC(CH<sub>3</sub>)<sub>2</sub>), 62.1 (COCH<sub>2</sub>), 55.8 (OCH<sub>3</sub>), 55.4 (CH<sub>2</sub>NH), 54.3, 54.2, 50.5 and 50.4 (piperazine), 29.3 ppm (OC(CH<sub>3</sub>)<sub>2</sub>); HPLC-MS: [A, 15%→40%], *t*<sub>R</sub>: 7.71 min (95%), MS (ES<sup>+</sup>, *m/z*) 462 [M+H]<sup>+</sup>; HRMS calcd for C<sub>26</sub>H<sub>31</sub>N<sub>5</sub>O<sub>3</sub>: 461.2426, found: 461.2421.

**1,4-Dihydro-7-methoxy-1-{2-[4-(2-methoxyphenyl)piperazinyl]acetamidomethyl}-4,4-dimethylchromeno[4,3-*c*]pyrazole (14a) and 2,4-dihydro-7-methoxy-2-{2-[4-(2-methoxyphenyl)piperazinyl]acetamidomethyl}-4,4-dimethylchromeno[4,3-*c*]pyrazole (14b).**

Compound **14a** was obtained as a white gummy solid (3% yield); <sup>1</sup>H-NMR (500 MHz, CDCl<sub>3</sub>) δ: 7.35 (d, *J* = 8.1 Hz, 1H, 9-H), 7.16 (s, 1H, 3-H), 6.71-6.59 (m, 4H, phenyl), 6.42 (dd, *J* = 8.1, 2.4 Hz, 1H, 8-H), 6.38 (d, *J* = 2.4 Hz, 1H, 6-H), 5.27 (s, 2H, CH<sub>2</sub>NH), 3.59 (s, 3H, OCH<sub>3</sub>), 3.54 (s, 3H, OCH<sub>3</sub>), 3.29 (s, 2H, COCH<sub>2</sub>), 3.10-3.03 (m, 4H, piperazine), 2.98-2.86 (m, 4H, piperazine), 1.69 ppm (s, 6H, OC(CH<sub>3</sub>)<sub>2</sub>); <sup>13</sup>C-NMR (126 MHz, CDCl<sub>3</sub>) δ: 175.0 (CO), 160.4 (7-C), 155.6 (5a-C), 155.1 (phenyl), 149.5 (phenyl), 147.1 (9b-C), 130.2 (3-C), 127.5 (9-C), 124.9 (3a-C), 118.7, 116.9, 116.3, 113.3 (4 C phenyl), 111.4 (9a-C), 106.8 (8-C), 104.2 (6-C), 75.8 (OC(CH<sub>3</sub>)<sub>2</sub>), 61.4 (COCH<sub>2</sub>), 55.9 (OCH<sub>3</sub>), 55.1 (OCH<sub>3</sub>), 54.0 (CH<sub>2</sub>NH), 53.7 and 51.3 (piperazine), 25.9 ppm (OC(CH<sub>3</sub>)<sub>2</sub>); HPLC-MS: [A, 15%→40%], *t*<sub>R</sub>: 7.35 min (93%), MS (ES<sup>+</sup>, *m/z*) 492 [M+H]<sup>+</sup>; HRMS calcd for C<sub>27</sub>H<sub>33</sub>N<sub>5</sub>O<sub>4</sub>: 491.2532, found: 491.2528. Compound **14b** was obtained as a yellow oil (8% yield); <sup>1</sup>H-NMR (500 MHz, CDCl<sub>3</sub>) δ: 7.04 (d, *J* = 7.5 Hz, 1H, 9-H), 6.91 (s, 1H, 3-H), 6.69-6.51 (m, 5H, 8-H, phenyl), 6.42 (d, *J* = 2.6 Hz, 1H, 6-H), 5.51 (s, 2H, CH<sub>2</sub>NH), 3.64 (s, 3H, OCH<sub>3</sub>), 3.59 (s, 3H, OCH<sub>3</sub>), 3.16 (s, 2H, COCH<sub>2</sub>), 2.92-2.89 (m, 4H, piperazine), 2.76-2.70 (m, 4H, piperazine), 1.54 ppm (s, 6H, OC(CH<sub>3</sub>)<sub>2</sub>); <sup>13</sup>C-NMR (126 MHz, CDCl<sub>3</sub>) δ: 173.2 (CO), 163.1 (7-C), 156.7 (5a-C), 153.1 (phenyl), 148.1 (phenyl), 144.9 (9b-C), 132.6 (3-C), 126.1 (9-C), 125.6 (3a-C), 120.9, 118.2, 117.5, 114.0 (4 C phenyl), 110.6 (9a-C), 109.4 (8-C), 106.0 (6-C), 75.3 (OC(CH<sub>3</sub>)<sub>2</sub>), 60.2 (COCH<sub>2</sub>), 56.8 (OCH<sub>3</sub>), 56.1 (OCH<sub>3</sub>), 54.6

(CH<sub>2</sub>NH), 52.5 and 50.7 (piperazine), 26.4 ppm (OC(CH<sub>3</sub>)<sub>2</sub>); HPLC-MS: [A, 15%→40%], *t<sub>R</sub>*: 7.17 min (95%), MS (ES<sup>+</sup>, *m/z*) 492 [M+H]<sup>+</sup>; HRMS calcd for C<sub>27</sub>H<sub>33</sub>N<sub>5</sub>O<sub>4</sub>: 491.2532, found: 491.2540.

**1-{2-[4-(2,3-Dimethylphenyl)piperazinyl]acetamidomethyl}-1,4-dihydro-7-methoxy-4,4-dimethylchromeno[4,3-*c*]pyrazole (15a) and 2-{2-[4-(2,3-dimethylphenyl)piperazinyl]acetamidomethyl}-2,4-dihydro-7-methoxy-4,4-**

**dimethylchromeno[4,3-*c*]pyrazole (15b).** Compound **15a** was obtained as a yellow oil (2% yield); <sup>1</sup>H-NMR (500 MHz, CDCl<sub>3</sub>) δ: 8.08-8.02 (bt, *J* = 6.4 Hz, 1H, NH), 7.76 (d, *J* = 8.1 Hz, 1H, 9-H), 7.50 (s, 1H, 3-H), 6.94 (t, *J* = 7.5 Hz, 1H, phenyl), 6.85 (d, *J* = 7.5 Hz, 1H, phenyl), 6.80 (d, *J* = 7.7 Hz, 1H, phenyl), 6.61 (dd, *J* = 8.1, 2.6 Hz, 1H, 8-H), 6.48 (d, *J* = 2.6 Hz, 1H, H-6), 5.61 (d, *J* = 6.4 Hz, 2H, CH<sub>2</sub>NH), 3.84 (s, 3H, OCH<sub>3</sub>), 3.08 (s, 2H, COCH<sub>2</sub>), 2.77-2.69 (m, 4H, piperazine), 2.64-2.59 (m, 4H, piperazine), 2.31 (s, 3H, CH<sub>3</sub>), 2.27 (s, 3H, CH<sub>3</sub>), 1.48 ppm (s, 6H, OC(CH<sub>3</sub>)<sub>2</sub>); <sup>13</sup>C-NMR (126 MHz, CDCl<sub>3</sub>) δ: 169.8 (CO), 162.4 (7-C), 156.0 (5a-C), 151.3 (phenyl), 144.2 (9b-C), 140.3 (v), 132.5 (3-C), 126.1 (9-C), 125.0 (C<sub>e</sub>), 123.9 (phenyl), 123.1 (phenyl), 121.8 (3a-C), 117.2 (phenyl), 109.8 (9a-C), 108.4 (8-C), 104.9 (6-C), 75.7 (OC(CH<sub>3</sub>)<sub>2</sub>), 61.3 (COCH<sub>2</sub>), 56.0 (OCH<sub>3</sub>), 54.7 (CH<sub>2</sub>NH), 53.3 and 51.9 (piperazine), 28.8 (OC(CH<sub>3</sub>)<sub>2</sub>), 19.7 (CH<sub>3</sub>), 14.1 ppm (CH<sub>3</sub>); HPLC-MS: [A, 15%→40%], *t<sub>R</sub>*: 9.47 min (92%), MS (ES<sup>+</sup>, *m/z*) 490 [M+H]<sup>+</sup>; HRMS calcd for C<sub>28</sub>H<sub>35</sub>N<sub>5</sub>O<sub>3</sub>: 489.2739, found: 489.2746. Compound **15b** was obtained as a white solid (4% yield); mp: 199-201 °C; <sup>1</sup>H-NMR (500 MHz, CDCl<sub>3</sub>) δ: 8.22-8.17 (br t, *J* = 6.9 Hz, 1H, NH), 7.62 (d, *J* = 8.5 Hz, 1H, 9-H), 7.42 (s, 1H, 3-H), 7.08 (t, *J* = 7.7 Hz, 1H, phenyl), 6.91 (d, *J* = 7.7 Hz, 1H, phenyl), 6.87 (d, *J* = 7.7 Hz, 1H, phenyl), 6.57 (dd, *J* = 8.5, 2.5 Hz, 1H, 8-H), 6.51 (d, *J* = 2.5 Hz, 1H, H-6), 5.54 (d, *J* = 6.9 Hz, 2H, CH<sub>2</sub>NH), 3.79 (s, 3H, OCH<sub>3</sub>), 3.11 (s, 2H, COCH<sub>2</sub>), 2.87 (t, *J* = 4.8 Hz, 4H, piperazine), 2.63 (t, *J* = 4.8 Hz, 4H,

piperazine), 2.25 (s, 3H, CH<sub>3</sub>), 2.18 (s, 3H, CH<sub>3</sub>), 1.58 ppm (s, 6H, OC(CH<sub>3</sub>)<sub>2</sub>); <sup>13</sup>C-NMR (126 MHz, CDCl<sub>3</sub>) δ: 171.5 (CO), 161.0 (7-C), 154.6 (5a-C), 151.1 (phenyl), 143.5 (9b-C), 138.0 (phenyl), 131.2 (3-C), 125.8 (9-C), 125.2 (phenyl), 124.7 (phenyl), 122.8(phenyl), 121.5 (3a-C), 116.6 (phenyl), 110.4 (9a-C), 108.0 (8-C), 103.0 (6-C), 76.5 (OC(CH<sub>3</sub>)<sub>2</sub>), 61.4 (COCH<sub>2</sub>), 55.3 (OCH<sub>3</sub>), 54.2 (CH<sub>2</sub>NH), 53.9 and 52.0 (piperazine), 29.1 (OC(CH<sub>3</sub>)<sub>2</sub>), 20.6 (CH<sub>3</sub>), 13.8 ppm (CH<sub>3</sub>); HPLC-MS: [A, 15%→40%], *t*<sub>R</sub>: 9.11 min (95%), MS (ES<sup>+</sup>, *m/z*) 490 [M+H]<sup>+</sup>; HRMS calcd for C<sub>28</sub>H<sub>35</sub>N<sub>5</sub>O<sub>3</sub>: 489.2739, found: 489.2750.

**1,4-Dihydro-7-methoxy-1-{2-[4-(4-methoxyphenyl)piperazinyl]acetamidomethyl}-4,4-dimethylchromeno[4,3-*c*]pyrazole (16).** Compound **16** was obtained as a yellow oil (14% yield); <sup>1</sup>H-NMR (500 MHz, CDCl<sub>3</sub>) δ: 7.50-7.48 (br t, *J* = 5.1 Hz, 1H, NH), 6.81-6.76 (m, 4H, 9-H, 3-H, phenyl), 6.76-6.68 (m, 2H, phenyl), 6.47 (dd, *J* = 8.5, 2.5 Hz, 1H, 8-H), 6.39 (d, *J* = 2.5 Hz, 1H, 6-H), 5.39 (d, *J* = 5.1 Hz, 2H, CH<sub>2</sub>NH), 3.68 (s, 3H, OCH<sub>3</sub>), 3.63 (s, 3H, OCH<sub>3</sub>), 3.01 (s, 2H, COCH<sub>2</sub>), 2.97-2.94 (m, 4H, piperazine), 2.55-2.47 (m, 4H, piperazine), 1.46 ppm (s, 6H, OC(CH<sub>3</sub>)<sub>2</sub>); <sup>13</sup>C-NMR (126 MHz, CDCl<sub>3</sub>) δ: 172.2 (CO), 161.2 (7-C), 154.6 (5a-C), 154.2 (C<sub>a</sub>), 145.2 (9b-C), 143.2 (C<sub>d</sub>), 125.1 (3-C), 122.4 (9-C), 120.9 (3a-C), 118.7 (2C phenyl), 113.8 (2C phenyl), 110.0 (9a-C), 107.3 (8-C), 102.7 (6-C), 76.1 (OC(CH<sub>3</sub>)<sub>2</sub>), 60.6 (COCH<sub>2</sub>), 54.4 (OCH<sub>3</sub>), 54.3 (OCH<sub>3</sub>), 53.9 (CH<sub>2</sub>NH), 52.9, 50.4 (piperazine), 27.8 ppm (OC(CH<sub>3</sub>)<sub>2</sub>); HPLC-MS: [A, 15%→40%], *t*<sub>R</sub>: 7.35 min (93%), MS (ES<sup>+</sup>, *m/z*) 492 [M+H]<sup>+</sup>; HRMS calcd for C<sub>27</sub>H<sub>33</sub>N<sub>5</sub>O<sub>4</sub>: 491.2532, found: 491.2524.

**1-(2-Bromoethyl)-1,4-dihydro-7-methoxy-4,4-dimethylchromeno[4,3-*c*]pyrazole (17a) and 2-(2-bromoethyl)-2,4-dihydro-7-methoxy-4,4-dimethylchromeno[4,3-*c*]pyrazole (17b).** A solution of **4** (0.23 g, 1.0 mmol) in anhydrous THF (8 mL) was added dropwise to a precooled suspension of sodium hydride (28 mg, 1.2 mmol) in anhydrous THF (1 mL) under nitrogen

atmosphere. The resulting mixture was stirred for 10 minutes at rt. 1,2-Dibromoethane (0.42 mL, 4.97 mmol) was added and the reaction mixture was refluxed for 4 h. The solvent was removed under vacuum and the crude was diluted in EtOAc, washed with water and extracted three times with EtOAc. The combined organic layers were dried over MgSO<sub>4</sub> and the solvent was removed under vacuum. Column chromatography on silica gel (hexane/EtOAc, 1:1) afforded the two isomers **17a** and **17b**. Compound **17a** was obtained as a yellow oil (75 mg, 20%); <sup>1</sup>H NMR (400 MHz, CDCl<sub>3</sub>) δ: 7.34 (d, *J* = 7.9 Hz, 1H, 9-H), 7.22 (s, 1H, 3-H), 6.50 (dd, *J* = 7.9, 2.4 Hz, 1H, 8-H), 6.43 (d, *J* = 2.4 Hz, 1H, 6-H), 4.61 (t, *J* = 6.6 Hz, 2H, 1'-H), 4.09 (t, *J* = 6.6 Hz, 2H, 2'-H), 3.92 (s, 3H, OCH<sub>3</sub>), 1.45 ppm (s, 6H, OC(CH<sub>3</sub>)<sub>2</sub>); <sup>13</sup>C-NMR (101 MHz, CDCl<sub>3</sub>) δ: 161.7 (7-C), 155.3 (5a-C), 144.7 (9b-C), 133.4 (3-C), 123.9 (9-C), 121.9 (3a -C), 108.5 (8-C), 103.4 (6-C), 101.8 (9a-C), 76.7 (OC(CH<sub>3</sub>)<sub>2</sub>), 59.3 (OCH<sub>3</sub>), 55.8 (1'-C), 29.6 (OC(CH<sub>3</sub>)<sub>2</sub>); 28.5 ppm (2'-C); HPLC-MS: [A, 30→95%], *t*<sub>R</sub>: 4.66 min, (94%); MS (ES<sup>+</sup>, *m/z*) 337 [M + H]<sup>+</sup>; HRMS calcd for C<sub>15</sub>H<sub>17</sub>BrN<sub>2</sub>O<sub>2</sub>: 336.0473, found: 336.0478. Compound **17b** was obtained as a yellow oil (0.19 g, 51%); <sup>1</sup>H-NMR (400 MHz, CDCl<sub>3</sub>) δ: 7.68 (d, *J* = 8.4 Hz, 1H, 9-H), 7.32 (s, 1H, 3-H), 6.63 (dd, *J* = 8.4, 2.5 Hz, 1H, 8-H), 6.58 (d, *J* = 2.5 Hz, 1H, 6-H), 4.54 (t, *J* = 6.5 Hz, 2H, 1'-H), 3.86 (s, 3H, OCH<sub>3</sub>), 3.80 (t, *J* = 6.5 Hz, 2H, 2'-H), 1.66 ppm (s, 6H, OC(CH<sub>3</sub>)<sub>2</sub>). <sup>13</sup>C-NMR (101 MHz, CDCl<sub>3</sub>) δ: 161.1 (7-C), 154.7 (5a-C), 143.8 (9b-C), 124.6 (3-C), 123.2 (9-C), 120.9 (3a -C), 110.9 (8-C), 108.1 (6-C), 103.2 (9a-C), 76.6 (OC(CH<sub>3</sub>)<sub>2</sub>), 55.5 (OCH<sub>3</sub>), 53.8 (1'-C), 30.7 (2'-C), 29.4 ppm (OC(CH<sub>3</sub>)<sub>2</sub>); HPLC-MS: [A, 30→95%], *t*<sub>R</sub>: 4.54 min, (96%); MS (ES<sup>+</sup>, *m/z*) 337 [M + H]<sup>+</sup>; HRMS calcd for C<sub>15</sub>H<sub>17</sub>BrN<sub>2</sub>O<sub>2</sub>: 336.0473, found: 336.0470.

**General procedure for the synthesis of acylpiperazinylethylchromenopyrazoles (18-24).** A mixture of the corresponding acyl piperazine (1 eq) and K<sub>2</sub>CO<sub>3</sub> (3 eq) was stirred 10 minutes at room temperature in THF. Then, the corresponding chromenopyrazole **17a** or **17b** (1 eq)

dissolved in THF was added. The resulting mixture was refluxed overnight. The solvent was evaporated, the crude was dissolved in EtOAc, washed with water and extracted three times with EtOAc. The organic layers were combined and dried over MgSO<sub>4</sub>, filtered and the solvent was evaporated under reduced pressure. The residue was purified by flash column chromatography performed on a Biotage Isolera One. The chromatography eluents and yields are indicated below for each reaction.

**1-{2-[4-(2-Furoyl)piperazinyl]ethyl}-1,4-dihydro-7-methoxy-4,4-dimethylchromeno[4,3-*c*]pyrazole (18a).** Flash column chromatography (hexane/EtOAc, 1:1) afforded **18a** as a white oil (25% yield); <sup>1</sup>H-NMR (CDCl<sub>3</sub>) δ: 7.57 (d, *J* = 8.5 Hz, 1H, 9-H), 7.33-7.28 (m, 1H, furoyl), 7.11 (s, 1H, 3-H), 6.96-6.92 (m, 1H, furoyl), 6.60 (dd, *J* = 8.5, 2.5 Hz, 1H, 8-H), 6.53 (d, *J* = 2.5 Hz, 1H, 6-H), 6.39-6.36 (m, 1H, furoyl), 4.22 (t, *J* = 6.6 Hz, 2H, 1'-H), 3.78 (s, 3H, OCH<sub>3</sub>), 3.39-3.21 (m, 4H, piperazine), 2.83 (t, *J* = 6.6 Hz, 2H, 2'-H), 2.72-2.64 (m, 4H, piperazine), 1.52 ppm (s, 6H, OC(CH<sub>3</sub>)<sub>2</sub>); <sup>13</sup>C-NMR (101 MHz, CDCl<sub>3</sub>) δ: 162.0 (CO), 155.6 (7-C), 153.1 (5a-C), 145.3 (9b-C), 142.6 (furoyl), 141.8 (furoyl), 124.1 (3-C), 123.2 (9-C), 121.3 (3a-C), 117.0, 112.2 (2C furoyl), 109.2 (9a -C), 108.4 (8-C), 103.2 (6-C), 76.1 (OC(CH<sub>3</sub>)<sub>2</sub>), 57.5 (OCH<sub>3</sub>), 55.1 (2'-C), 54.1 and 50.7 (piperazine), 49.5 (1'-C), 28.9 ppm (OC(CH<sub>3</sub>)<sub>2</sub>); HPLC-MS: [A, 15%→95%], *t<sub>R</sub>*: 2.88 min (94%), MS (ES<sup>+</sup>, *m/z*) 437 [M+H]<sup>+</sup>; HRMS calcd for C<sub>24</sub>H<sub>28</sub>N<sub>4</sub>O<sub>4</sub>: 436.2110, found: 436.2107.

**2-{2-[4-(2-Furoyl)piperazinyl]ethyl}-2,4-dihydro-7-methoxy-4,4-dimethylchromeno[4,3-*c*]pyrazole (18b).** Flash column chromatography (EtOAc/MeOH, 98:2) afforded **18b** as a pale yellow oil (24 % yield); <sup>1</sup>H-NMR (400 MHz, CDCl<sub>3</sub>) δ: 7.61 (d, *J* = 8.4 Hz, 1H, 9-H), 7.48-7.45 (m, 1H, furoyl), 7.18 (s, 1H, 3-H), 7.00-6.94 (m, 1H, furoyl), 6.54 (dd, *J* = 8.4, 2.5 Hz, 1H, 8-H), 6.50 (d, *J* = 2.5 Hz, 1H, 6-H), 6.46-6.44 (m, 1H, furoyl), 4.23 (t, *J* = 6.5 Hz, 2H, 1'-H), 3.76-3.62

(br s, 7H, OCH<sub>3</sub>, piperazine), 2.86 (t, *J* = 6.5 Hz, 2H, 2'-H), 2.70-2.66 (m, 4H, piperazine), 1.58 ppm (s, 6H, OC(CH<sub>3</sub>)<sub>2</sub>); <sup>13</sup>C-NMR (101 MHz, CDCl<sub>3</sub>) δ: 160.9 (CO), 159.3 (7-C), 154.5 (5a-C), 148.0 (9b-C), 143.9 (furoyl), 142.9 (furoyl), 124.2 (3-C), 123.1 (9-C), 121.0 (3a-C), 116.7, 111.5 (2C furoyl), 111.2 (9a-C), 108.0 (8-C), 103.2 (6-C), 76.7 (OC(CH<sub>3</sub>)<sub>2</sub>), 58.0 (OCH<sub>3</sub>), 55.5 (2'-C), 53.6 and 51.3 (piperazine), 50.4 (1'-C), 29.5 ppm (OC(CH<sub>3</sub>)<sub>2</sub>); HPLC-MS: [A, 15%→95%], *t*<sub>R</sub>: 2.91 min (100%), MS (ES<sup>+</sup>, *m/z*) 437 [M+H]<sup>+</sup>; HRMS calcd for C<sub>24</sub>H<sub>28</sub>N<sub>4</sub>O<sub>4</sub>: 436.2110, found: 436.2121.

**1-[2-(4-Benzoyl-piperazinyl)ethyl]-1,4-dihydro-7-methoxy-4,4-dimethylchromeno[4,3-c]pyrazole (19a).** Flash column chromatography (hexane/EtOAc, 1:1) yielded **19a** as a yellow gummy solid (30 % yield); <sup>1</sup>H-RMN (CDCl<sub>3</sub>) δ: 7.55 (d, *J* = 8.4 Hz, 1H, 9-H), 7.38-7.29 (m, 5H, phenyl), 7.13 (s, 1H, 3-H), 6.49 (dd, *J* = 8.4, 2.5 Hz, 1H, 8-H), 6.44 (d, *J* = 2.5 Hz, 1H, 6-H), 4.41 (t, *J* = 6.7 Hz, 2H, 1'-H), 3.73 (s, 3H, OCH<sub>3</sub>), 3.41-3.26 (m, 4H, piperazine), 2.81 (t, *J* = 6.7 Hz, 2H, 2'-H), 2.59-2.37 (m, 4H, piperazine), 1.52 ppm (s, 6H, OC(CH<sub>3</sub>)<sub>2</sub>); <sup>13</sup>C-NMR (101 MHz, CDCl<sub>3</sub>) δ: 170.3 (CO), 165.1 (7-C), 160.7 (5a-C), 154.3 (9b-C), 130.2 (phenyl), 129.7 (phenyl), 128.5, 127.1 (4C phenyl), 124.4 (3-C), 123.9 (9-C), 122.8 (3a-C), 107.9 (9a -C), 107.6 (8-C), 103.0 (6-C), 76.4 (OC(CH<sub>3</sub>)<sub>2</sub>), 57.8 (OCH<sub>3</sub>), 55.4 (2'-C), 55.3 and 53.6 (piperazine), 50.1 (1'-C), 29.2. ppm (OC(CH<sub>3</sub>)<sub>2</sub>); HPLC-MS: [A, 15%→95%], *t*<sub>R</sub>: 3.05 min (97%), MS (ES<sup>+</sup>, *m/z*) 447 [M+H]<sup>+</sup>; HRMS calcd for C<sub>26</sub>H<sub>30</sub>N<sub>4</sub>O<sub>3</sub>: 446.2317, found: 446.2324.

**2-[2-(4-Benzoyl-piperazinyl)ethyl]-2,4-dihydro-7-methoxy-4,4-dimethylchromeno[4,3-c]pyrazole (19b).** Flash column chromatography (EtOAc/MeOH, 95:5) gave **19b** as a yellow solid (81 % yield); mp: 161-162 °C; <sup>1</sup>H-NMR (400 MHz, CDCl<sub>3</sub>) δ: 7.62 (d, *J* = 8.4 Hz, 1H, 9-H), 7.46-7.32 (m, 5H, phenyl), 7.17 (s, 1H, 3-H), 6.55 (dd, *J* = 8.4, 2.5 Hz, 1H, 8-H), 6.50 (d, *J* = 2.5 Hz, 1H, 6-H), 4.23 (t, *J* = 6.6 Hz, 2H, 1'-H), 3.79 (s, 3H, OCH<sub>3</sub>), 3.41-3.20 (m, 4H,



piperazine), 2.87 (t,  $J = 6.6$  Hz, 2H, 2'-H), 2.73-2.60 (m, 4H, piperazine), 1.58 ppm (s, 6H, OC(CH<sub>3</sub>)<sub>2</sub>); <sup>13</sup>C-NMR (101 MHz, CDCl<sub>3</sub>)  $\delta$ : 170.4 (CO), 160.8 (7-C), 154.5 (5a-C), 142.9 (9b-C), 135.8 (phenyl), 129.9 (phenyl), 128.6, 127.1 (4C phenyl), 124.1 (3-C), 123.0 (9-C), 120.9 (3a-C), 111.1 (9a -C), 107.9 (8-C), 103.1 (6-C), 76.6 (OC(CH<sub>3</sub>)<sub>2</sub>), 57.9 (OCH<sub>3</sub>), 55.4 (2'-C), 53.7 and 50.2 (piperazine), 47.9 (1'-C), 29.4 ppm (OC(CH<sub>3</sub>)<sub>2</sub>); HPLC-MS: [A, 15%→95%],  $t_R$ : 3.08 min (100%), MS (ES<sup>+</sup>,  $m/z$ ) 447 [M+H]<sup>+</sup>; HRMS calcd for C<sub>26</sub>H<sub>30</sub>N<sub>4</sub>O<sub>3</sub>: 446.2317, found: 446.2311.

**1,4-Dihydro-7-methoxy-4,4-dimethyl-1-{2-[4-(2-thenoyl)piperazinyl]ethyl}-chromeno[4,3-c]pyrazole (20a).** Flash column chromatography (hexane/EtOAc, 1:9) yielded **20a** as a yellow gummy solid (23 % yield); <sup>1</sup>H-NMR (400 MHz, CDCl<sub>3</sub>)  $\delta$ : 7.49 (d,  $J = 8.8$  Hz, 1H, 9-H), 7.44 (dd,  $J = 5.0, 1.2$  Hz, 1H, thenoyl), 7.28 (s, 1H, 3-H), 7.23-7.21 (m, 1H, thenoyl), 7.03 (dd,  $J = 5.0, 3.6$  Hz, 1H, thenoyl), 6.61-6.58 (m, 1H, 8-H), 6.57 (d,  $J = 2.6$  Hz, 1H, 6-H), 4.54 (t,  $J = 7.1$  Hz, 2H, 1'-H), 3.82 (s, 3H, OCH<sub>3</sub>), 3.77-3.64 (m, 4H, piperazine), 2.93-2.87 (m, 2H, 2'-H), 2.67-2.43 (m, 4H, piperazine), 1.58 ppm (s, 6H, OC(CH<sub>3</sub>)<sub>2</sub>); <sup>13</sup>C-NMR (101 MHz, CDCl<sub>3</sub>)  $\delta$ : 163.7 (CO), 161.0 (7-C), 154.6 (5a-C), 150.3 (9b-C), 137.1 (thenoyl), 132.8, 129.1, 128.9 (thenoyl), 126.9 (3-C), 122.7 (9-C), 121.4 (3a-C), 109.1 (9a -C), 107.9 (8-C), 104.1 (6-C), 76.4 (OC(CH<sub>3</sub>)<sub>2</sub>), 57.4 (OCH<sub>3</sub>), 55.6 (2'-C), 53.6 and 51.3 (piperazine), 49.5 (1'-C), 28.6 ppm (OC(CH<sub>3</sub>)<sub>2</sub>); HPLC-MS: [A, 15%→95%],  $t_R$ : 3.22 min (97%), MS (ES<sup>+</sup>,  $m/z$ ) 453 [M+H]<sup>+</sup>; HRMS calcd for C<sub>24</sub>H<sub>28</sub>N<sub>4</sub>O<sub>3</sub>S: 452.1882, found: 452.1891.

**2,4-Dihydro-7-methoxy-4,4-dimethyl-2-{2-[4-(2-thenoyl)piperazinyl]ethyl}-chromeno[4,3-c]pyrazole (20b).** Flash column chromatography (EtOAc/MeOH, 98:2) afforded **20b** as a yellow solid (55 % yield); mp: 163-165 °C; <sup>1</sup>H-NMR (400 MHz, CDCl<sub>3</sub>)  $\delta$ : 7.62 (d,  $J = 8.4$  Hz, 1H, 9-H), 7.44 (dd,  $J = 5.0, 1.2$  Hz, 1H, thenoyl), 7.25-7.23 (m, 1H, thenoyl), 7.20 (s, 1H, 3-H), 7.03

(dd,  $J = 5.0, 3.6$  Hz, 1H, thenoyl), 6.55 (dd,  $J = 8.4, 2.5$  Hz, 1H, 8-H), 6.51 (d,  $J = 2.5$  Hz, 1H, 6-H), 4.27 (t,  $J = 6.5$  Hz, 2H, 1'-H), 3.79 (s, 3H, OCH<sub>3</sub>), 3.78-3.72 (m, 4H, piperazine), 3.01-2.91 (m, 2H, 2'-H), 2.63-2.43 (m, 4H, piperazine), 1.59 ppm (s, 6H, OC(CH<sub>3</sub>)<sub>2</sub>); <sup>13</sup>C-NMR (101 MHz, CDCl<sub>3</sub>)  $\delta$ : 163.8 (CO), 161.0 (7-C), 154.6 (5a-C), 143.1 (9b-C), 137.0 (thenoyl), 129.1, 128.9, and 126.9 (thenoyl), 124.3 (3-C), 123.1 (9-C), 121.0 (3a-C), 111.1 (9a -C), 108.0 (8-C), 103.2 (6-C), 76.7 (OC(CH<sub>3</sub>)<sub>2</sub>), 57.9 (OCH<sub>3</sub>), 55.5 (2'-C), 53.5 and 50.2 (piperazine), 46.1 (1'-C), 29.5 ppm (OC(CH<sub>3</sub>)<sub>2</sub>); HPLC-MS: [A, 15%→95%],  $t_R$ : 3.03 min (100%), MS (ES<sup>+</sup>,  $m/z$ ) 453 [M+H]<sup>+</sup>; HRMS calcd for C<sub>24</sub>H<sub>28</sub>N<sub>4</sub>O<sub>3</sub>S: 452.1882, found: 452.1889.

**2,4-Dihydro-7-methoxy-4,4-dimethyl-2-[2-(4-phenoxyacetyl)piperazinyl]ethyl-chromeno[4,3-c]pyrazole (21).** Flash column chromatography (EtOAc/MeOH, 95:5) afforded **21** as an orange solid (38 % yield); mp: 177-179 °C; <sup>1</sup>H-NMR (500 MHz, CD<sub>3</sub>OD)  $\delta$ : 7.56 (d,  $J = 8.5$  Hz, 1H, 9-H), 7.52 (s, 1H, 3-H), 7.31-7.21 (m, 2H, phenoxy), 7.00-6.90 (m, 3H, phenoxy), 6.56 (dd,  $J = 8.5, 2.5$  Hz, 1H, 8-H), 6.48 (d,  $J = 2.5$  Hz, 1H, 6-H), 4.76 (s, 2H, OCH<sub>2</sub>), 4.26 (t,  $J = 6.4$  Hz, 2H, 1'-H), 3.77 (s, 3H, OCH<sub>3</sub>), 3.63-3.50 (m, 4H, piperazine), 2.84 (t,  $J = 6.4$  Hz, 2H, 2'-H), 2.56-2.46 (m, 4H, piperazine), 1.56 ppm (s, 6H, OC(CH<sub>3</sub>)<sub>2</sub>); <sup>13</sup>C-NMR (126 MHz, CD<sub>3</sub>OD)  $\delta$ : 167.4 (CO), 161.1 (7-C), 158.0 (phenoxy), 154.5 (5a-C), 142.5 (9b-C), 129.1 (2C phenoxy), 125.4 (3-C), 122.3 (9-C), 121.1 (phenoxy), 120.5 (9-C), 114.3 (2C phenoxy), 110.4 (9a-C), 107.2 (8-C), 102.8 (6-C), 76.2 (OC(CH<sub>3</sub>)<sub>2</sub>), 66.1 (OCH<sub>2</sub>), 57.2 (OCH<sub>3</sub>), 54.3 (2'-C), 52.8 and 52.3 (piperazine), 49.1 (1'-C), 44.7 and 43.7 (piperazine), 28.0 ppm (OC(CH<sub>3</sub>)<sub>2</sub>); HPLC-MS: [A, 15%→95%],  $t_R$ : 3.24 min (100%), MS (ES<sup>+</sup>,  $m/z$ ) 477 [M+H]<sup>+</sup>; HRMS calcd for C<sub>27</sub>H<sub>32</sub>N<sub>4</sub>O<sub>4</sub>: 476.2423, found: 476.2427.

**2,4-Dihydro-7-methoxy-4,4-dimethyl-2-{2-[4-(2-tetrahydrofuroyl)piperazinyl]ethyl}-chromeno[4,3-c]pyrazole (22).** Flash column chromatography (EtOAc/MeOH, 98:2) furnished

**22** as a yellow solid (36 % yield); mp: 158-160 °C; <sup>1</sup>H-NMR (500 MHz, CD<sub>3</sub>OD) δ: 7.46 (d, *J* = 8.5 Hz, 1H, 9-H), 7.43 (s, 1H, 3-H), 6.46 (dd, *J* = 8.5, 2.5 Hz, 1H, 8-H), 6.38 (d, *J* = 2.5 Hz, 1H, 6-H), 4.67- 4.54 (m, 1H, tetrahydrofuroyl), 4.17 (t, *J* = 6.5 Hz, 2H, 1'-H), 3.83-3.81 (m, 1H, tetrahydrofuroyl), 3.76-3.70 (m, 1H, tetrahydrofuroyl), 3.68 (s, 3H, OCH<sub>3</sub>), 3.55-3.39 (m, 4H, piperazine), 2.76 (t, *J* = 6.5 Hz, 2H, 2'-H), 2.46-2.33 (m, 4H, piperazine), 2.12-1.99 (m, 1H, tetrahydrofuroyl), 1.95-1.86 (m, 1H, tetrahydrofuroyl), 1.85-1.75 (m, 2H, tetrahydrofuroyl), 1.47 ppm (s, 6H, OC(CH<sub>3</sub>)<sub>2</sub>); <sup>13</sup>C-NMR (126 MHz, CD<sub>3</sub>OD) δ: 171.3 (CO), 161.1 (7-C), 154.5 (5a-C), 142.5 (9b-C), 125.4 (3-C), 122.3 (9-C), 120.5 (3a-C), 110.4 (9a-C), 107.2 (8-C), 102.8 (6-C), 76.2 (tetrahydrofuroyl), 75.2 (OC(CH<sub>3</sub>)<sub>2</sub>), 68.7 (tetrahydrofuroyl), 57.2 (OCH<sub>3</sub>), 54.3 (2'-C), 52.9, 52.3 (piperazine), 47.5 (1'-C), 44.9 and 43.7 (piperazine), 28.8 (tetrahydrofuroyl), 28.0 (OC(CH<sub>3</sub>)<sub>2</sub>), 25.1 ppm (tetrahydrofuroyl); HPLC-MS: [A, 15%→95%], *t*<sub>R</sub>: 2.98 min (95%), MS (ES<sup>+</sup>, *m/z*) 441 [M+H]<sup>+</sup>; HRMS calcd for C<sub>24</sub>H<sub>32</sub>N<sub>4</sub>O<sub>4</sub>: 440.2423, found: 440.2436.

**2-[2-(4-Cyclohexylcarbonylpiperazinyl)ethyl]-2,4-dihydro-7-methoxy-4,4-dimethylchromeno[4,3-*c*]pyrazole (23).** Flash column chromatography (EtOAc/MeOH, 95:5) yielded **23** as a yellow solid (62 % yield); mp: 151-152 °C; <sup>1</sup>H-NMR (400 MHz, CDCl<sub>3</sub>) δ: 7.63 (d, *J* = 8.5 Hz, 1H, 9-H), 7.18 (s, 1H, 3-H), 6.56 (dd, *J* = 8.5, 2.5 Hz, 1H, 8-H), 6.51 (d, *J* = 2.4 Hz, 1H, 6-H), 4.23 (t, *J* = 6.6 Hz, 2H, cyclohexyl), 3.79 (s, 3H, OCH<sub>3</sub>), 3.66-3.39 (m, 4H, piperazine), 2.85 (t, *J* = 6.6 Hz, 2H, 2'-H), 2.54-2.35 (m, 4H, piperazine), 1.82-1.75 (m, 1H, cyclohexyl), 1.73-1.61 (m, 4H, cyclohexyl), 1.59 (s, 6H, OC(CH<sub>3</sub>)<sub>2</sub>), 1.57-1.42 ppm (m, 6H, cyclohexyl); <sup>13</sup>C-NMR (101 MHz, CDCl<sub>3</sub>) δ: 174.8 (CO), 160.9 (7-C), 154.6 (5a-C), 143.0 (9b-C), 124.2 (3-C), 123.1 (9-C), 121.0 (3a-C), 111.2 (9a-C), 108.0 (8-C), 103.2 (6-C), 76.7 (OC(CH<sub>3</sub>)<sub>2</sub>), 58.0 (OCH<sub>3</sub>), 55.5 (2'-C), 53.2 and 50.3 (piperazine), 45.6 (1'-C), 41.7 (cyclohexyl), 30.6 (cyclohexyl), 29.6 (OC(CH<sub>3</sub>)<sub>2</sub>), 26.1 ppm (cyclohexyl); HPLC-MS: [A,

15%→95%],  $t_R$ : 3.19 min (100%), MS (ES<sup>+</sup>,  $m/z$ ) 453 [M+H]<sup>+</sup>; HRMS calcd for C<sub>26</sub>H<sub>36</sub>N<sub>4</sub>O<sub>3</sub>: 452.2787, found: 452.2773.

**2,4-Dihydro-7-methoxy-4,4-dimethyl-2-[2-(4-pivaloylpiperazinyl)ethyl]-chromeno[4,3-c]pyrazole (24).** Flash column chromatography (EtOAc/MeOH, 95:5) gave **3.19** as a yellow gummy solid (32 % yield); <sup>1</sup>H-NMR (400 MHz, CDCl<sub>3</sub>) δ: 7.62 (d,  $J$  = 8.4 Hz, 1H, 9-H), 7.18 (s, 1H, 3-H), 6.55 (dd,  $J$  = 8.4, 2.5 Hz, 1H, 8-H), 6.51 (d,  $J$  = 2.5 Hz, 1H, 6-H), 4.23 (t,  $J$  = 6.6 Hz, 2H, 1'-H), 3.79 (s, 3H, OCH<sub>3</sub>), 3.63 (t,  $J$  = 5.0 Hz, 4H, piperazine), 2.84 (t,  $J$  = 6.6 Hz, 2H, 2'-H), 2.46 (t,  $J$  = 5.0 Hz, 4H, piperazine), 1.59 (s, 6H, OC(CH<sub>3</sub>)<sub>2</sub>), 1.26 (s, 9H, C(CH<sub>3</sub>)<sub>3</sub>); <sup>13</sup>C-NMR (101 MHz, CDCl<sub>3</sub>) δ: 176.5 (CO), 160.9 (7-C), 154.6 (5a-C), 142.9 (9b-C), 124.2 (3-C), 123.1 (9-C), 121.0 (3a-C), 111.2 (9a -C), 108.0 (8-C), 103.2 (6-C), 76.7 (OC(CH<sub>3</sub>)<sub>2</sub>), 58.0 (OCH<sub>3</sub>), 55.5 (2'-C), 53.6, 50.2 (piperazine), 45.3 (1'-C), 38.8 (C(CH<sub>3</sub>)<sub>3</sub>), 29.5 (OC(CH<sub>3</sub>)<sub>2</sub>), 28.6 ppm (C(CH<sub>3</sub>)<sub>3</sub>); HPLC-MS: [A, 15%→95%],  $t_R$ : 2.99 min (99%), MS (ES<sup>+</sup>,  $m/z$ ) 427 [M+H]<sup>+</sup>; HRMS calcd for C<sub>24</sub>H<sub>34</sub>N<sub>4</sub>O<sub>3</sub>: 426.2630, found: 426.2618.

***In silico* ADME calculations.** A set of 34 physico-chemical descriptors was computed using QikProp version 3.5 integrated in Maestro (Schrödinger, LLC, New York, USA). The QikProp descriptors are shown in table 3. The 3D conformations used in the calculation of QikProp descriptors were generated using the program Spartan '08 (Wave function, Inc., Irvine CA) as follows: the structure of each molecule was built from the fragment library available in the program. Then, *ab initio* energy minimizations of each structure at the Hartree-Fock 6-31G\* level were performed. A conformational search was next implemented using Molecular Mechanics (Monte Carlo method) followed by a minimization of the energy of each conformer calculated at the Hartree-Fock 6-31G\* level. The global minimum energy conformer of each compound was used as input for ADME studies with QikProp.

## **Pharmacological assays.**

**xCELLigence assays.** Normal HEK293 and hGPR55-HEK293<sup>23</sup> cells were maintained at 37 °C with 5% CO<sub>2</sub> in  $\alpha$ -MEM supplemented with 10% FBS, 100 IU/mL Penicillin, 100ug/mL Streptomycin and 2 mM Glutamine. The xCELLigence RTCA instrument (ACEA Biosciences; San Diego, CA) is housed within the incubator at all times allowing all experiments to be performed at 37 °C with 5% CO<sub>2</sub>. E-plates (ACEA Biosciences; San Diego, CA) with microelectrodes integrated into the bottom of the wells allowed measurement of impedance at the electrode-cell interface. In preparation for the experiment, cells were grown to 80% confluence in flasks, harvested by trypsinisation and then seeded into 96 well E-plates at a density of  $5 \times 10^4$  cells per well in duplicate. Before the addition of cells to the plate, a background reading was obtained by adding 100  $\mu$ l of serum free media to each well in order to adjust for any discrepancies between wells (wells with a cell index reading above or below 0.01 were not used for experiments). Cellular impedance was measured every 30 minutes overnight in order to monitor cell attachment and subsequent proliferation. The following day the cells were switched to serum free media (100  $\mu$ l  $\alpha$ -MEM without FBS) for 5 hours, the time taken for cellular impedance to re-stabilize in normal HEK293 and GPR55-HEK293 cells. L- $\alpha$ -lysophosphatidylinositol (LPI) derived from soybean was purchased from Avanti Polar Lipids. All ligands were prepared in serum free media with a final concentration of DMSO at 0.1% (agonist studies) or 0.2% (antagonist studies). Compounds were tested at concentrations from 1 nM to 10  $\mu$ M. The experiment is started immediately after the addition of test compounds to the wells (10  $\mu$ l per well). To ensure consistency within the analysis, all experiments were normalized to the point directly before the addition of test compounds. Once normalized, the minimum cell index (dose dependent decrease found to be 5 minutes for all the compounds) was

obtained and converted to a percentage decrease in cellular impedance. Dose response curves were generated using GraphPad PRISM software in order to calculate  $EC_{50}$  and  $E_{max}$  values. Full concentration–response curves for LPI in presence and absence of the compounds were determined by coadministration of the test compounds at 1  $\mu$ M (or vehicle) and different concentrations of the standard agonist.

**Cannabinoid receptor binding analysis.** Membranes purified from cells transfected with human  $CB_1$  or  $CB_2$  receptors (RBHCB1M400UA and RBXCB2M400UA) were supplied by Perkin-Elmer Life and Analytical Sciences (Boston, MA). The protein concentration was 8  $\mu$ g/well for the  $CB_1$  receptor membranes and 4  $\mu$ g/well for the  $CB_2$  receptor. The binding buffer was 50 mM TrisCl, 5 mM  $MgCl_2$ , 2.5 mM EDTA, 0.5 mg/mL BSA (pH = 7.4) for  $CB_1$ , and 50 mM TrisCl, 5 mM  $MgCl_2$ , 2.5 mM EGTA, 1 mg/mL BSA (pH = 7.5) for  $CB_2$ . The radioligand was [ $^3H$ ]-CP55940 (PerkinElmer) used at a concentration of membrane  $K_D \times 0.8$  nM, and the final incubation volume was 200  $\mu$ L for  $CB_1$  and 600  $\mu$ L for  $CB_2$ . 96-Well plates and the tubes necessary for the experiment were previously siliconized with Sigmacote (Sigma). Membranes were resuspended in the corresponding buffer and were incubated (90 min at 30 °C) with the radioligand and the different compounds at a high concentration (40  $\mu$ M) with the purpose to determine the % of radioligand displacement. Only in those cases in which radioligand displacement at these conditions were greater than 70%, a complete competition curve with different compound concentrations ( $10^{-4}$ - $10^{-11}$  M) was carried out to obtain the  $K_i$  values. Non-specific binding was determined with 10  $\mu$ M WIN55212-2 and total radioligand binding by incubation with the membranes in absence of any compound. Filtration was performed by a Harvester<sup>®</sup> filtermate (Perkin-Elmer) with Filtermat A GF/C filters pretreated with polyethylenimine 0.05%. After filtering, the filter was washed nine times with binding buffer,

dried and a melt-on scintillation sheet (Meltilex A, Perkin Elmer) was melted onto it. Then, radioactivity was quantified by a liquid scintillation spectrophotometer (Wallac MicroBeta Trilux, Perkin-Elmer). Competition binding data were analyzed by using GraphPad Prism program and  $K_i$  values are expressed as mean  $\pm$  SEM of at least three experiments performed in triplicate for each point.

**[ $^{35}$ S]-GTP $\gamma$ S Binding analysis.** [ $^{35}$ S]-GTP $\gamma$ S binding analysis of compound **24** was performed using CB<sub>2</sub>R-containing membranes (HTS020M2, Eurofins Discovery Services). For this purpose, membranes (5  $\mu$ g/well) were permeabilized by addition of saponin (Sigma-Aldrich), then mixed with 0.3 nM [ $^{35}$ S]-GTP $\gamma$ S (Perkin-Elmer) and 10  $\mu$ M GDP (Sigma-Aldrich) in 20 mM HEPES (Sigma-Aldrich) buffer containing 100 mM NaCl (Merck) and 10 mM MgCl<sub>2</sub> (Merck), at pH 7.4. 30 nM CP55,940 (Sigma-Aldrich) and increasing concentrations of compound **24** (from  $10^{-11}$  to  $10^{-4}$  M) were added in a final volume of 100  $\mu$ l and incubated for 30 min at 30 °C. The non-specific signal was measured with 10  $\mu$ M GTP $\gamma$ S (Sigma-Aldrich). All 96-well plates and the tubes necessary for the experiment were previously silanized with Sigmacote (Sigma-Aldrich). The reaction was terminated by rapid vacuum filtration with a filtermate Harvester apparatus (Perkin-Elmer) through Filtermat A GF/C filters. The filters were rinsed nine times with washing buffer (10 mM sodium phosphate, pH 7.4), and left to dry, and melt-on scintillation pads (Meltilex A, Perkin Elmer) were melted onto them. The bound radioactivity was quantified by liquid scintillation spectrophotometer (Wallac MicroBeta Trilux, PerkinElmer). Data were analyzed by nonlinear regression analysis of sigmoidal dose- response curves using GraphPad Prism 5.02 (GraphPad, San Diego, CA). EC<sub>50</sub> and E<sub>max</sub> values are expressed as mean  $\pm$  SEM of at least three independent experiments performed in triplicate.

## AUTHOR INFORMATION

### **Corresponding Authors**

\*For N.J.: phone, +34-91-562-2900; fax, +34-564-4853; E-mail: [nadine@iqm.csic.es](mailto:nadine@iqm.csic.es)

\*For R.R.: phone, +416-978-2723; fax, +416-978-6395; E-mail: [ruth.ross@utoronto.ca](mailto:ruth.ross@utoronto.ca)

### **Present Addresses**

†Justesa Imagen, Avda. San Pablo, 27, 28823 Coslada, Madrid, Spain.

### **Author Contributions**

The manuscript was written through contributions of all authors. All authors have given approval to the final version of the manuscript.

## ACKNOWLEDGMENT

Financial supports by Spanish Grants from the Spanish Ministry MINECO SAF2012-40075-C02-02, from CAM S2010/BMD-2308. P.M. is recipient of a fellowship JAE-Pre-2010-01119 from Junta para la Ampliación de Estudios co-financed by FSE. L.W. is funded by the University of Toronto. P.M., P.G. and N.J. dedicate this paper to Prof. Dr. José Elguero on the occasion of his 80<sup>th</sup> birthday.

## ABBREVIATIONS



CBRs, cannabinoid receptors; CB<sub>1</sub>R, cannabinoid receptor type 1; CB<sub>2</sub>R, cannabinoid receptor type 2; SAR, structure-activity-relationship; LPI, lysophosphatidylinositol; ADME, administration, distribution, metabolism, excretion.

## REFERENCES

- (1) Sawzdargo, M.; Nguyen, T.; Lee, D. K.; Lynch, K. R.; Cheng, R.; Heng, H. H. Q.; George, S. R.; O'Dowd, B. F. Identification and cloning of three novel human G protein-coupled receptor genes GPR52, GPR53 and GPR55: GPR55 is extensively expressed in human brain. *Mol. Brain Res.* **1999**, *64*, 193–198.
- (2) Drmota, T.; Greasley, P.; Groblewski, T. Screening assays for cannabinoid- ligand-type modulators of GPR55. AstraZeneca. **2004**, WO2004/0748844.
- (3) Brown, A. J.; Wise, A. Identification of modulators of GPR55 activity. Glaxosmithkline. **2001**, WO2001/86305A2.
- (4) Zhao, P.; Abood, M. E. GPR55 and GPR35 and their relationship to cannabinoid and lysophospholipid receptors. *Life Sci.* **2013**, *92*, 453–457.
- (5) Shore, D. M.; Reggio, P. H. The therapeutic potential of orphan GPCRs, GPR35 and GPR55. *Front. Pharmacol.* **2015**, *6*, 1–22.
- (6) Ross, R. A. The enigmatic pharmacology of GPR55. *Trends Pharmacol. Sci.* **2009**, *30*, 156–163.
- (7) Ryberg, E.; Larsson, N.; Sjögren, S.; Hjorth, S.; Hermansson, N.-O.; Leonova, J.; Elebring, T.; Nilsson, K.; Drmota, T.; Greasley, P. J. The orphan receptor GPR55 is a novel cannabinoid receptor. *Br. J. Pharmacol.* **2007**, *152*, 1092–1101.
- (8) Johns, D. G.; Behm, D. J.; Walker, D. J.; Ao, Z.; Shapland, E. M.; Daniels, D. A.; Riddick, M.; Dowell, S.; Staton, P. C.; Green, P.; Shabon, U.; Bao, W.; Aiyar, N.; Yue, T.-L.; Brown, A. J.; Morrison, A. D.; Douglas, S. A. The novel endocannabinoid receptor GPR55 is activated by atypical cannabinoids but does not mediate their vasodilator effects. *Br. J. Pharmacol.* **2007**, *152*, 825–831.
- (9) GPR18, GPR55 and GPR119: GPR55. IUPHAR/BPS Guide to Pharmacology <http://www.guidetopharmacology.org/GRAC/FamilyDisp>.
- (10) Pertwee, R. G.; Howlett, A. C.; Abood, M. E.; Alexander, S. P. H.; Marzo, V. Di; Elphick, M. R.; Greasley, P. J.; Hansen, H. S.; Kunos, G. International Union of Basic and Clinical Pharmacology . LXXIX . Cannabinoid Receptors and Their Ligands : Beyond CB<sub>1</sub> and CB<sub>2</sub>. **2010**, *62*, 588–631.

- (11) Sharir, H.; Abood, M. E. Pharmacological characterization of GPR55, a putative cannabinoid receptor. *Pharmacol. Ther.* **2010**, *126*, 301–313.
- (12) Moriconi, A.; Cerbara, I.; Maccarrone, M.; Topai, A. GPR55: Current knowledge and future perspectives of a purported “Type-3” cannabinoid receptor. *Curr. Med. Chem.* **2010**, *17*, 1411–1429.
- (13) Nevalainen, T.; Irving, A. J. GPR55, a lysophosphatidylinositol receptor with cannabinoid sensitivity? *Curr. Top. Med. Chem.* **2010**, *1*, 799–813.
- (14) Elbegdorj, O.; Westkaemper, R. B.; Zhang, Y. A homology modeling study toward the understanding of three-dimensional structure and putative pharmacological profile of the G-protein coupled receptor GPR55. *J. Mol. Graph. Model.* **2013**, *39*, 50–60.
- (15) Staton, P. C.; Hatcher, J. P.; Walker, D. J.; Morrison, A. D.; Shapland, E. M.; Hughes, J. P.; Chong, E.; Mander, P. K.; Green, P. J.; Billinton, A.; Fulleylove, M.; Lancaster, H. C.; Smith, J. C.; Bailey, L. T.; Wise, A.; Brown, A. J.; Richardson, J. C.; Chessell, I. P. The putative cannabinoid receptor GPR55 plays a role in mechanical hyperalgesia associated with inflammatory and neuropathic pain. *Pain* **2008**, *139*, 225–236.
- (16) Moreno-Navarrete, J. M.; Catalán, V.; Whyte, L.; Díaz-Arteaga, A.; Vázquez-Martínez, R.; Rotellar, F.; Guzmán, R.; Gómez-Ambrosi, J.; Pulido, M. R.; Russell, W. R.; Imbernón, M.; Ross, R. a; Malagón, M. M.; Dieguez, C.; Fernández-Real, J. M.; Frühbeck, G.; Nogueiras, R. The L- $\alpha$ -lysophosphatidylinositol/GPR55 system and its potential role in human obesity. *Diabetes* **2012**, *61*, 281–291.
- (17) Daly, C. J.; Ross, R. a; Whyte, J.; Henstridge, C. M.; Irving, a J.; McGrath, J. C. Fluorescent ligand binding reveals heterogeneous distribution of adrenoceptors and “cannabinoid-like” receptors in small arteries. *Br. J. Pharmacol.* **2010**, *159*, 787–796.
- (18) Whyte, L. S.; Ryberg, E.; Sims, N. A.; Ridge, S. A.; Mackie, K.; Greasley, P. J.; Ross, R. A.; Rogers, M. J. The putative cannabinoid receptor GPR55 affects osteoclast function in vitro and bone mass in vivo. *Proc. Natl. Acad. Sci. U. S. A.* **2009**, *106*, 16511–16516.
- (19) Leyva-Illades, D.; Demorrow, S. Orphan G protein receptor GPR55 as an emerging target in cancer therapy and management. *Cancer Manag. Res.* **2013**, *5*, 147–155.
- (20) Ford, L. A.; Roelofs, A. J.; Anavi-Goffer, S.; Mowat, L.; Simpson, D. G.; Irving, A. J.; Rogers, M. J.; Rajnicek, A. M.; Ross, R. A. A role for L-alpha-lysophosphatidylinositol and GPR55 in the modulation of migration, orientation and polarization of human breast cancer cells. *Br. J. Pharmacol.* **2010**, *160*, 762–771.
- (21) Andradas, C.; Caffarel, M. M.; Pérez-Gómez, E.; Salazar, M.; Lorente, M.; Velasco, G.; Guzmán, M.; Sánchez, C. The orphan G protein-coupled receptor GPR55 promotes cancer cell proliferation via ERK. *Oncogene* **2011**, *30*, 245–252.
- (22) Anavi-Goffer, S.; Baillie, G.; Irving, A. J.; Gertsch, J.; Greig, I. R.; Pertwee, R. G.; Ross, R. A. Modulation of L- $\alpha$ -lysophosphatidylinositol/GPR55 mitogen-activated protein kinase (MAPK) signaling by cannabinoids. *J. Biol. Chem.* **2012**, *287*, 91–104.

- (23) Henstridge, C. M.; Balenga, N. A. B.; Ford, L. A.; Ross, R. A.; Waldhoer, M.; Irving, A. J. The GPR55 ligand L- $\alpha$ -lysophosphatidylinositol promotes RhoA-dependent Ca<sup>2+</sup> signaling and NFAT activation. *FASEB J.* **2009**, *23*, 183–193.
- (24) Ross, R. A. L- $\alpha$ -lysophosphatidylinositol meets GPR55: a deadly relationship. *Trends Pharmacol. Sci.* **2011**, *32*, 265–269.
- (25) Oka, S.; Nakajima, K.; Yamashita, A.; Kishimoto, S.; Sugiura, T. Identification of GPR55 as a lysophosphatidylinositol receptor. *Biochem. Biophys. Res. Commun.* **2007**, *362*, 928–934.
- (26) Oka, S.; Toshida, T.; Maruyama, K.; Nakajima, K.; Yamashita, A.; Sugiura, T. 2-Arachidonoyl-sn-glycero-3-phosphoinositol: a possible natural ligand for GPR55. *J. Biochem.* **2009**, *145*, 13–20.
- (27) Yin, H.; Chu, A.; Li, W.; Wang, B.; Shelton, F.; Otero, F.; Nguyen, D. G.; Caldwell, J. S.; Chen, Y. A. Lipid G protein-coupled receptor ligand identification using beta-arrestin PathHunter assay. *J. Biol. Chem.* **2009**, *284*, 12328–12338.
- (28) Pertwee, R. G. GPR55: a new member of the cannabinoid receptor clan? *Br. J. Pharmacol.* **2007**, *152*, 984–986.
- (29) Kapur, A.; Zhao, P.; Sharir, H.; Bai, Y.; Caron, M. G.; Barak, L. S.; Abood, M. E. Atypical responsiveness of the orphan receptor GPR55 to cannabinoid ligands. *J. Biol. Chem.* **2009**, *284*, 29817–29827.
- (30) Lauckner, J. E.; Jensen, J. B.; Chen, H.-Y.; Lu, H.-C.; Hille, B.; Mackie, K. GPR55 is a cannabinoid receptor that increases intracellular calcium and inhibits M current. *Proc. Natl. Acad. Sci. U. S. A.* **2008**, *105*, 2699–26704.
- (31) Heynen-Genel, S.; Dahl, R.; Shi, S.; Milan, L.; Hariharan, S.; Bravo, Y.; Sergienko, E.; Hedrick, M.; Dad, S.; Stonich, D.; Su, Y.; Vicchiarelli, M.; Mangravita-Novo, A.; Smith, L. H.; Chung, T. D.; Sharir, H.; Barak, L. S.; Abood, M. E. Screening for Selective Ligands for GPR55 - Agonists <http://www.ncbi.nlm.nih.gov/books/NBK66152/> (accessed Jun 10, 2015).
- (32) Heynen-Genel, S.; Dahl, R.; Shi, S.; Milan, L.; Hariharan, S.; Sergienko, E.; Hedrick, M.; Dad, S.; Stonich, D.; Su, Y.; Vicchiarelli, M.; Mangravita-Novo, A.; Smith, L. H.; Chung, T. D.; Sharir, H.; Caron, M. G.; Barak, L. S.; Abood, M. E. Screening for Selective Ligands for GPR55 - Antagonists <http://www.ncbi.nlm.nih.gov/books/NBK66153/> (accessed Jun 10, 2015).
- (33) Brown, A. J.; Daniels, D. a; Kassim, M.; Brown, S.; Haslam, C. P.; Terrell, V. R.; Brown, J.; Nichols, P. L.; Staton, P. C.; Wise, A.; Dowell, S. J. Pharmacology of GPR55 in yeast and identification of GSK494581A as a mixed-activity glycine transporter subtype 1 inhibitor and GPR55 agonist. *J. Pharmacol. Exp. Ther.* **2011**, *337*, 236–246.
- (34) Kargl, J.; Brown, A. J.; Andersen, L.; Dorn, G.; Schicho, R.; Waldhoer, M.; Heinemann, A. A selective antagonist reveals a potential role of G protein-coupled receptor 55 in platelet and endothelial cell function. *J. Pharmacol. Exp. Ther.* **2013**, *346*, 54–66.

- (35) Paul, R. K.; Wnorowski, A.; Gonzalez-Mariscal, I.; Nayak, S. K.; Pajak, K.; Moaddel, R.; Indig, F. E.; Bernier, M.; Wainer, I. W. (R,R')-4'-methoxy-1-naphthylfenoterol targets GPR55-mediated ligand internalization and impairs cancer cell motility. *Biochem. Pharmacol.* **2014**, *87*, 547–561.
- (36) Cumella, J.; Hernández-Folgado, L.; Girón, R.; Sánchez, E.; Morales, P.; Hurst, D. P.; Gómez-Cañas, M.; Gómez-Ruiz, M.; Pinto, D. C. G. A.; Goya, P.; Reggio, P. H.; Martin, M. I.; Fernández-Ruiz, J.; Silva, A. M. S.; Jagerovic, N. Chromenopyrazoles: non-psychoactive and selective CB1 cannabinoid agonists with peripheral antinociceptive properties. *ChemMedChem* **2012**, *7*, 452–463.
- (37) Morales, P.; Blasco-Benito, S.; Andradas, C.; Gómez-Cañas, M.; Flores, J. M.; Goya, P.; Fernández-Ruiz, J.; Sánchez, C.; Jagerovic, N. A selective, non-toxic CB2 cannabinoid o-quinone with in vivo activity against triple negative breast cancer. *J. Med. Chem.* **2015**, *58*, 2256–2264.
- (38) Morales, P.; Vara, D.; Gómez-Cañas, M.; Zúñiga, M. C.; Olea-Azar, C.; Goya, P.; Fernández-Ruiz, J.; Díaz-Laviada, I.; Jagerovic, N. Synthetic cannabinoid quinones: Preparation, in vitro antiproliferative effects and in vivo prostate antitumor activity. *Eur. J. Med. Chem.* **2013**, *70*, 111–119.
- (39) Kotsikorou, E.; Sharir, H.; Shore, D. M.; Hurst, D. P.; Lynch, D. L.; Madrigal, K. E.; Heynen-genel, S.; Milan, L. B.; Chung, T. D. Y.; Seltzman, H. H.; Bai, Y.; Caron, M. G.; Barak, L. S.; Croatt, M. P.; Abood, M. E.; Reggio, P. H. Identification of the GPR55 Antagonist Binding Site Using a Novel Set of High-Potency GPR55 Selective Ligands. *Biochemistry* **2013**, *52*, 9456–9468.
- (40) Kotsikorou, E.; Lynch, D. L.; Abood, M. E.; Reggio, P. H. Lipid bilayer molecular dynamics study of lipid-derived agonists of the putative cannabinoid receptor, GPR55. *Chem. Phys. Lipids* **2011**, *164*, 131–143.
- (41) Kotsikorou, E.; Madrigal, K. E.; Hurst, D. P.; Sharir, H.; Lynch, D. L.; Heynen-Genel, S.; Milan, L. B.; Chung, T. D. Y.; Seltzman, H. H.; Bai, Y.; Caron, M. G.; Barak, L.; Abood, M. E.; Reggio, P. H. Identification of the GPR55 agonist binding site using a novel set of high-potency GPR55 selective ligands. *Biochemistry* **2011**, *50*, 5633–5647.
- (42) Childers, S. R.; Deadwyler, S. A. Role of cyclic AMP in the actions of cannabinoid receptors. *Biochem. Pharmacol.* **1996**, *52*, 819–827.
- (43) Bonhaus, D. W.; Chang, L. K.; Kwan, J.; Martin, G. R. Dual activation and inhibition of adenylyl cyclase by cannabinoid receptor agonists: Evidence for agonist-specific trafficking of intracellular responses. *J. Pharmacol. Exp. Ther.* **1998**, *287*, 884–888.
- (44) Waldeck-Weiermair, M.; Zoratti, C.; Osibow, K.; Balenga, N.; Goessnitzer, E.; Waldhoer, M.; Malli, R.; Graier, W. F. Integrin clustering enables anandamide-induced Ca<sup>2+</sup> signaling in endothelial cells via GPR55 by protection against CB1-receptor-triggered repression. *J. Cell Sci.* **2008**, *121*, 1704–1717.

- (45) Atienzar, F. A.; Gerets, H.; Tilmant, K.; Toussaint, G.; Dhalluin, S. Evaluation of impedance-based label-free technology as a tool for pharmacology and toxicology investigations. *Biosensors* **2013**, *3*, 132–156.
- (46) Stolwijk, J. a.; Matrougui, K.; Renken, C. W.; Trebak, M. Impedance analysis of GPCR-mediated changes in endothelial barrier function: overview and fundamental considerations for stable and reproducible measurements. *Pflügers Arch. - Eur. J. Physiol.* **2014**, DOI 10.1007/s00424-014-1674-0.
- (47) Ke, N.; Nguyen, K.; Irelan, J.; Abassi, Y. A. Multidimensional GPCR profiling and screening using impedance-based label-free and real-time assay. In *G Protein-Coupled Receptor Screening Assays*; Prazeres, D. M. F.; Martins, S. A. M., Eds.; New York, 2015; pp. 215–226.
- (48) Ke, N.; Nguyen, K.; Irelan, J.; Abassi, Y. A. Multidimensional GPCR profiling and screening using impedance-based label-free and real-time assay. *Methods Mol. Biol.* **2015**, *1272*, 215–26.
- (49) Henstridge, C. M.; Balenga, N. A.; Schröder, R.; Kargl, J. K.; Platzer, W.; Martini, L.; Arthur, S.; Penman, J.; Whistler, J. L.; Kostenis, E.; Waldhoer, M.; Irving, A. J. GPR55 ligands promote receptor coupling to multiple signalling pathways. *Br. J. Pharmacol.* **2010**, *160*, 604–614.
- (50) Lauren, D. W.; Irving, A.; Ross, R.; Proceeding from Experimental Biology Meeting EB2015 Boston USA Pharmacological Profiling of Lysophosphatidylinositol Species at GPR55 Using xCELLigence Cellular Impedance Analysis. *FASEB J* **2015**, *29*, 772.13.
- (51) Whyte, L.; Irving, A.; Ruth A., R. Pharmacological Profiling of GPR55 ligands Using Cellular Impedance Analysis. *25th Annu. Symp. Int. Cannabinoid Res. Soc.* **2015**, P97.
- (52) Zhu, M.; Kim, M. H.; Lee, S.; Bae, S. J.; Kim, S. H.; Park, S. B. Discovery of novel benzopyranyl tetracycles that act as inhibitors of osteoclastogenesis induced by receptor activator of NF- $\kappa$ B ligand. *J. Med. Chem.* **2010**, *53*, 8760–8764.
- (53) Camps, F.; Coll, J.; Messeguer, A.; Pericás, M. A.; Ricart, S.; Bowers, W. S.; Soderlund, D. M. An Improved Procedure for the Preparation of 2,2-Dimethyl-4-chromanones. *Synthesis (Stuttg).* **1980**, *1980*, 725–727.
- (54) An, H.; Eum, S.-J.; Koh, M.; Lee, S. K.; Park, S. B. Diversity-oriented synthesis of privileged benzopyranyl heterocycles from s-cis-enones. *J. Org. Chem.* **2008**, *73*, 1752–1761.
- (55) Brown, R. E.; Shavel, J. J. Substituted Benzopyranopyrazoles **1971**, Patent US19690826656.
- (56) Scott, C. W.; Peters, M. F. Label-free whole-cell assays: expanding the scope of GPCR screening. *Drug Discov. Today* **2010**, *15*, 704–716.
- (57) Whyte, L.; Russell, W.; Ross, R. A. Production of lysophosphatidylinositol species and GPR55 mediated signaling in osteoclasts. In *ICRS 23rd Annual Symposium*; 2013; p. 179.

- (58) Yamashita, A.; Oka, S.; Tanikawa, T.; Hayashi, Y.; Nemoto-Sasaki, Y.; Sugiura, T. The actions and metabolism of lysophosphatidylinositol, an endogenous agonist for GPR55. *Prostaglandins Other Lipid Mediat.* **2013**, *107*, 103–116.
- (59) Piñeiro, R.; Falasca, M. Lysophosphatidylinositol signalling: New wine from an old bottle. *Biochim. Biophys. Acta - Mol. Cell Biol. Lipids* **2012**, *1821*, 694–705.
- (60) Balenga, N. A.; Martínez-Pinilla, E.; Kargl, J.; Schröder, R.; Peinhaupt, M.; Platzer, W.; Bálint, Z.; Zamarbide, M.; Dopeso-Reyes, I.; Ricobaraza, A.; Pérez-Ortiz, J. M.; Kostenis, E.; Waldhoer, M.; Heinemann, A.; Franco, R. Heteromerization of GPR55 and cannabinoid CB2 receptors modulates signaling. *Br. J. Pharmacol.* **2014**, *171*, 5387–5406.
- (61) Moreno, E.; Andradas, C.; Medrano, M.; Caffarel, M. M.; Pérez-Gómez, E.; Blasco-Benito, S.; Gómez-Cañas, M.; Pazos, M. R.; Irving, A. J.; Lluís, C.; Canela, E. I.; Fernández-Ruiz, J.; Guzmán, M.; McCormick, P. J.; Sánchez, C. Targeting CB2-GPR55 Receptor Heteromers Modulates Cancer Cell Signaling. *J. Biol. Chem.* **2014**, *289*, 21960–21972.

## Table of Contents Graphic

